REDUCTION OF INHERENT MERCURY EMISSIONS IN PC COMBUSTION

Final Technical Report

DOE Grant No. DE-FG22-95PC95216--09

Department of Mechanical Engineering
Box 352600
University of Washington
Seattle, Washington 98195-2600

August 26, 2000

Period of Performance: June 29, 1995 to December 28, 1999

Authors: John C. Kramlich and Rebecca N. Sliger

Contracting Officer's Representative: Anthony E. Mayne
U.S. Department of Energy
National Energy Technology Laboratory
P.O. Box 10940
Pittsburgh, Pennsylvania 15236-0940

Period Covered by Report: June 29, 1995 to December 28, 1999

Disclaimer

Abstract

Oxidized mercury has been shown to be more easily removed from power plant flue gas by existing air pollution control equipment (*e.g.,* wet scrubbers) than elemental mercury. The factors that determine how mercury is converted to the oxidized form in practical systems are, however, unknown. The present research focuses on developing an elementary, homogeneous mechanism that describes the oxidation of mercury by chlorine species as it occurs in practical furnaces. The goal is to use this mechanism (1) as a component in an overall homogeneous/ heterogeneous mechanism that describes mercury behavior, and (2) to suggest low cost/low impact means of promoting mercury oxidation in furnaces. The results suggest an important role for $Hg+Cl \rightarrow HgCl$ and $HgCl+Cl \rightarrow HgCl_2$. Here, the Cl is derived by radical attack on HCl in the high-temperature environment. The results suggest that the oxidation occurs during the time that the gases cool to room temperature. The high Cl concentrations from the flame persist into the quench region and provide for the oxidation of Hg to $HgCl_2$ under lower temperatures where the products are stable. Under this mechanism, no significant $HgCl_2$ is actually present at the higher temperatures where oxidized mercury is often reported in the literature (*e.g.,* 900°C). Instead, all oxidation occurs as these gases are quenched. The results suggest that means of promoting Cl concentrations in the furnace will increase oxidation.

Table of Contents

List of Figures

List of Tables

Executive Summary

Mercury vapor emissions from the combustion process have emerged as one of the major challenges presented to the electric utility industry by the Clean Air Act Amendments of 1990. Most of the emissions control measures that have been proposed appear to be very costly. Mercury is, however, at least partially captured by equipment designed to control other pollutants, particularly wet flue gas desulfurization systems (FGD). Field data show that the mercury entering FGD systems in the oxidized state is much more easily captured than that which enters in the elemental state. Field data also show a rough correlation between the chlorine content of the coal and the degree of oxidation of the mercury. Thus, while oxidized mercury is desirable since it is more easily captured, the mechanism that leads to oxidation and the means of promoting oxidation are not yet known.

Both homogeneous and heterogeneous oxidation processes occur, but the exact mechanisms and the relative importance of these to oxidation in practical systems are unknown. Given the correlation between chlorine and oxidation, HCl has become the principal species of interest. The data with respect to oxidation of mercury by HCl present a number of contradictions and uncertainties, however. These include:

- Equilibrium predicts that oxidized mercury will be favored only at lower temperatures (<500°C). Data, however, consistently suggest oxidation occurs only at high temperatures (*i.e.,* oxidation increases with temperature right up to the maximum temperatures examined experimentally, 900-1000°C).
- The amount of oxidation observed in various researchers' work differs substantially, even for similar residence times, temperatures and HCl concentrations. It appears that the lack of CO_2 and water vapor in the reacting gas tends to increase oxidation.
- Homogeneous oxidation must involve a series of elementary reaction steps. These have not yet been defined.

The goal of the work reported here is the development of an elementary homogeneous mechanism for the oxidation of mercury in the presence of HCl. This is then used to address the uncertainties listed above.

Experimental data were obtained on the influence of temperature, HCl concentration and mercury concentration on the percent of mercury that is oxidized. The results are consistent with other experiments conducted in real flue gas: (1) oxidation increases with higher temperatures, (2) oxidation increases with HCl concentration, (3) percentage oxidation is independent of mercury concentration, and (4) the oxidation extents are much lower than for experiments conducted in artificial atmospheres that are free of CO_2 and water vapor.

A detailed examination of the possible elementary pathways suggests that the principal reactions are likely to be:

$$Hg + Cl \rightarrow HgCl$$
$$HgCl + Cl \rightarrow HgCl_2$$

The Cl is generated from HCl via:

$$OH + HCl \rightarrow Cl + H_2O$$

The kinetics do not predict any significant HgCl or $HgCl_2$ concentration at high temperature, however, due to the instability of HgCl and $HgCl_2$. Instead, they suggest that an experiment run at 900-1000°C appears to give significant oxidation due to the following scenario:

- In the high-temperature reaction zone, Cl concentrations are essentially equilibrated.
- These gases are withdrawn from the reactor and pass through a cool-down region as they approach the mercury measurement system, which is at room temperature.
- During cool-down, the equilibrium chlorine atom concentration drops dramatically, but the actual concentration remains higher due to kinetic constraints on the recombination reaction: $Cl+Cl+M \rightarrow Cl_2+M$.
- As the gases cool, this high Cl concentration is available to react with Hg under conditions where the oxidized products are stable. This leads to the oxidation occurring during the thermal quench of the sampled gases, rather than in the high temperature reactor.

This suggests why oxidation is apparently reported at high temperatures, in contradiction to equilibrium, *i.e.,* that oxidation occurs during the cool down that always precedes the measurement system, not within the high-temperature reactor. The same process occurs in boilers, with the oxidation taking place as the gases are cooled via heat extraction before reaching the air pollution control equipment (albeit at a slower cooling rate than in the sample system quench).

The mechanism shows that in the absence of water vapor, equilibrium Cl atom concentrations increase by at least an order of magnitude. This suggests that an experiment run in the absence of water vapor would show much more oxidation than the corresponding experiment run under flue gas. This could explain why those experiments run under artificial atmospheres show more oxidation relative to those run under flue gas. These results can be used to hypothesize means to enhance oxidation within the boiler environment.

Papers generated under this grant are listed here:

Sliger, R. N., D. J. Going, and J. C. Kramlich: Kinetic investigation of the high-temperature oxidation of mercury by chlorine species. Paper 98F-18. *Fall 1998 Meeting of the Western State Section/The Combustion Institute*, Seattle, WA (October 1998).

Sliger, R. N., D. J. Going and, J. C. Kramlich: Mercury oxidation in furnaces: pathways, promotion and implications. *Air Pollution: Mercury, Trace Metals, and Air Toxics*, Tyson's Corner, VA (December 1998).

Sliger, R. N., J. C. Kramlich, and N. M. Marinov: Development of a chemical kinetic model for the homogeneous oxidation of mercury by chlorine species. Paper 99F-72. *Fall 1999 Meeting of the Western States Section/The Combustion Institute*, Irvine, CA (October 1999).

Sliger, R. N., J. C. Kramlich, N. M. Marinov: Development of an elementary homogeneous mercury oxidation mechanism. *93rd Annual Meeting of the Air & Waste Management Association,* Salt Lake City, UT (June 2000).

Sliger, R. N., J. C. Kramlich, and N. M. Marinov: Towards the development of a chemical kinetic model for the homogeneous oxidation of mercury by chlorine species. *Fuel Processing Technology* **65,** 423-438 (2000).

1.0 Introduction

The use of fossil fuels for electric power generation is responsible for a large portion of U.S. anthropogenic mercury emissions. At present, the environmental impact of these emissions remains uncertain, especially when compared to the relatively large rate at which mercury naturally enters the atmosphere. Power producers may, however, become subject to regulation in the near future under the 1990 Clean Air Act Amendments. The technical response to these potential regulations remains unclear, and the power producers may be faced with very costly custom control measures.

Field testing has shown the following with respect to mercury:

- The fraction of the original mercury in the coal that is emitted varies considerably between different combustion facilities.
- Mercury is emitted in both the elemental and divalent forms (the latter usually being termed "oxidized" mercury).
- Divalent mercury is much more easily captured in existing air pollution control equipment (*e.g.,* FGD wet scrubbers). Since divalent mercury is water-soluble, it is presumed to have a better chance of interacting with scrubbing liquids or solid surfaces near the end of the flue gas path.
- The fraction of divalent mercury tends to increase with increasing chlorine levels in the fuel. This clearly indicates a critical role for chlorine in the oxidation mechanism.

Thus, promoting mercury oxidation is one means of promoting reduced emissions. The mechanisms of oxidation, however, remain unclear. Purely homogeneous oxidation has been demonstrated. At the same time, many common surfaces (carbonaceous coal char, mineral-based fly ash) have shown activity for oxidation, reduction, and capture. The apparent complexity of the overall oxidation mechanism is mirrored in the wide variability of oxidation extents observed in the field data. This variability presents both a challenge and an opportunity. The challenge involves understanding the complex processes that govern oxidation. The opportunity is to make use of this mechanistic understanding to find inexpensive and easy means of promoting oxidation.

The work presented here focuses on developing a chemical kinetic mechanism for the homogeneous oxidation of mercury by chlorine species. An accurate homogeneous model is a necessary component in any overall model of mercury oxidation (*i.e.,* one cannot have an accurate heterogeneous model without considering all the concurrent gas-phase reactions). In addition, the insight gained by understanding the rate-limiting steps in the oxidation process (*i.e.,* finding the oxidation bottlenecks) offers the opportunity to identify simple means to promote oxidation.

The following sections provide a detailed technical background for the present work, culminating in a listing of the open issues we wish to address. We then discuss the experimental work and

the chemical kinetic mechanism development. Finally, we present the implications of our findings.

2.0 Background

2.1 Mercury Sources, Fates, and Impacts

Mercury cycles in and out of the atmosphere due to both natural and anthropogenic processes. The reservoir of mercury available for this cycle has increased over time as humans have extracted mercury fixed in minerals and released them into the environment via use in fungicides, in batteries, in burning of fuels, *etc*. The U.S. Environmental Protection Agency, in their "Mercury Report to Congress" estimates that 5500 tons of mercury annually enter the atmosphere from all global sources, both natural and anthropogenic (Environmental Protection Agency, 1997). These sources include soil outgassing, evaporation from bodies of water, release by vegetation, release by wildfires, and geothermal venting (Pai *et al.,* 2000). U.S. anthropogenic sources are estimated by the EPA to be 158 tons per year. A more recent estimate places this figure at 176 metric tons (193 English tons) (Pai *et al.,* 2000). Of this amount, 32% is estimated to be associated with waste incineration and 26% with coal and oil combustion. Thus, mercury emissions from U.S.-based fossil fuel combustion account for approximately 0.91% of the total global mercury flux into the atmosphere.

Mobile mercury (*i.e.,* mercury capable of cycling in and out of the atmosphere) exists in the environment in three forms: (1) elemental mercury, (2) divalent mercury, and (3) organic mercury (predominantly methylmercury: CH_3Hg). Most of the naturally-released mercury is in the elemental form, while anthropogenic mercury is released in both the elemental and divalent forms. Elemental mercury is relatively inert, and has an atmospheric lifetime of the order of one year (Fthenakis *et al.,* 1995). In the atmosphere it is slowly oxidized by O_3, NO_3 radical, and H_2O_2 (Lin and Pehkonen, 1999), which leads to rapid wet deposition. Alternately, the element can be lost due to dry deposition. The slowness of both the dry deposition and atmospheric oxidation processes leads to the long atmospheric lifetime, and thus elemental mercury can disperse widely before becoming deposited. Divalent mercury remains in the atmosphere for only 5-14 days (Carpo, 1997; Bergan *et al.,* 1999). The oxidized form is water-soluble and is easily washed out of the air by rainwater. Its deposition occurs much closer to the source due to its shorter atmospheric lifetime. Once deposited it is available for re-emission into the atmosphere as part of the cycle.

Both elemental and oxidized mercury are relatively easily eliminated from the body, and neither tends to bioaccumulate. In the aquatic environment, however, oxidized mercury is converted to methylmercury by bacteria, and methylmercury is a powerful bioaccumulant. As such, it concentrates into species at the top of the food chain (*i.e.,* the largest fish). The consumption of these fish is the most important pathway for mercury to enter the human population. Although the nervous system is sensitive to all forms of mercury, organic forms, such as methylmercury, are the most dangerous because they are fat soluble, allowing more mercury to reach the brain. Exposure to high amounts of mercury can permanently damage the brain, kidneys and a developing fetus. Effects on the brain may result in irritability, shyness, tremors, changes in

vision or hearing and memory problems (Agency for Toxic Substances and Disease Registry, 1995).

Establishing maximum safe levels of mercury intake has been very difficult due to lack of data and the long time required for chronic symptoms to become apparent. The most well documented cases involve epidemics of mercury poisoning following high-dose exposures to methylmercury in Japan (fish contamination) and Iraq (grain poisoning). These demonstrated that under high-dose, acute poisoning conditions, the most significant health concern is to a developing fetus. Dietary methylmercury is almost completely absorbed into the blood and distributed to all tissues including the brain. In the case of a pregnant woman, it also readily passes through the placenta to the fetus and fetal brain.

A considerable amount of uncertainty is associated with extrapolating these high-dose poisoning episodes to maximum safe dose levels for long-term exposure. The reference dose (RfD) is an amount of methylmercury which may be ingested daily throughout the lifetime without adverse health effects in humans, including sensitive subpopulations. At or below the RfD, exposures are expected to be safe. The risk of exposures above the RfD is uncertain, but risk increases as exposures to methylmercury increase (Environmental Protection Agency, 1997). Extrapolating from the high dose exposures that occurred in the Iraq incident, the U.S. EPA derived a RfD for methylmercury of 0.1 μg/kg body weight/day (this corresponds to 0.17 g of Hg as methylmercury over a 70-year lifetime for a 70 kg person). Currently two large studies in the Seychelle Islands and the Faroe Islands are being conducted to examine fetal exposure to methylmercury in fish-consuming populations. These studies may lead to a change in the RfD for methylmercury (Environmental Protection Agency, 1997).

As mentioned above, the primary pathway for human and wildlife exposure to methylmercury is fish consumption. However, the effect of anthropogenic sources on methylmercury concentrations in fish is less clear. Certain marine species tend to have higher mercury contents, but it is difficult to argue that these are strongly influenced by land-based fossil fuel combustion. The small percentage of the total atmospheric burden contributed by coal combustion and the large volume of mercury present in the ocean relative to that in the atmosphere all suggest that fossil fuel combustion is a small contribution to marine fish mercury contamination. Freshwater fish are much more likely to be influenced by mercury pollution (*i.e.,* washout of oxidized mercury from the air in the region immediately downwind of a source). However, given the current scientific understanding of the environmental fate and transport of this element, it is not possible to quantify how much of the methylmercury in freshwater fish is a result of emissions as opposed to natural sources. Therefore, the change in methylmercury concentration in fish due to a drop in anthropogenic mercury emissions cannot be accurately predicted (Environmental Protection Agency, 1997). Thus, the scientific basis needed to support regulation has not yet been demonstrated.

2.2 Mercury in Coal

The presence of toxic trace metals in coal was recognized at an early date. Early research showed that most of these metals are concentrated in the heaviest gravity fraction, implying that they are associated with mineral matter (Cavallaro *et al.,* 1978). Thus, physical coal cleaning is capable of significantly reducing the heavy metal content. Although some mercury is associated with pyrite, coal cleaning generally has not been as effective at removing mercury (Boren and Wan, 1990; Akers and Dospay, 1993, 1994; Devito *et al*., 1994). For example, the results of Devito *et al*. (1994) show only 30-40 percent removal during physical coal cleaning, as compared to 75-85 percent for the other trace elements and the minerals as a whole. This suggests that mercury is associated with the organic fraction to a greater degree than the other heavy metals.

The mercury concentration in raw coal varies widely, although most coals have mercury values within a range of a factor of 6. Reported values for U.S. bituminous coals range from 0.01-3.3 ppm (mass) with an average of 0.21 ppm (Liu, 1998). Values for anthracite average 0.23 ppm. Lower average values (<0.1 ppm) have been reported by Brown *et al.* (1999). Thus, the exact amount of mercury in the average U.S. coal remains somewhat uncertain, and thus total emissions from coal-based fossil power consumption is also somewhat uncertain. EPA is presently gathering data to develop a more firm figure (see Section 2.7).

2.3 Summary of Field Data

During combustion all the mercury contained in the coal is released into the vapor phase as elemental mercury (Rizeq *et al.*, 1994). A portion may oxidize before the exhaust point, and a portion may be captured in ash handling equipment or flue gas desulfurization equipment. The remaining mercury results in an emission of 5-70 $\mu g/Nm^3$ (Brown *et al.,* 1999). Measurements show that coal burning plants emit anywhere from 5% to 95% of the mercury contained in the coal (Jones, 1994).

There is a substantial variation in the concentration of elemental vs. oxidized mercury measured upstream of the air pollution control equipment (Brown *et al.,* 1999). A rough correlation has been noted between the amount of chlorine present in the fuel and the fraction of mercury present in the oxidized form (see Figure 2.1), but these data show considerable scatter and it appears that fuel rank, ash properties and combustor type all play a role in governing oxidation. The role of chlorine in promoting oxidation is a principal focus of the present work, and will be discussed in some detail later.

Pollution control devices are not designed to retain mercury. In some cases, however, they are moderately effective in removing mercury from the flue gas. Studies show a wide variety of mercury emission control using conventional air pollution devices. A summary of the effects of air pollution control devices on mercury emissions is shown in Table 2.1 (Jones, 1994). Although results vary from one study to the next, speciation of the mercury (*i.e.,* oxidized or elemental) appears to be one of the most significant factors affecting the efficiency of the

mercury removal. As mentioned above, oxidized mercury is water-soluble and it has a slightly lower vapor pressure compared to elemental under the temperatures present in air pollution control devices. Since conventional flue-gas cleanup technologies are reasonably effective in controlling oxidized mercury and poor in controlling elemental mercury, an understanding of the factors that control the speciation of mercury as it enters the air pollution control devices is critical (Senior *et al.*, 1997).

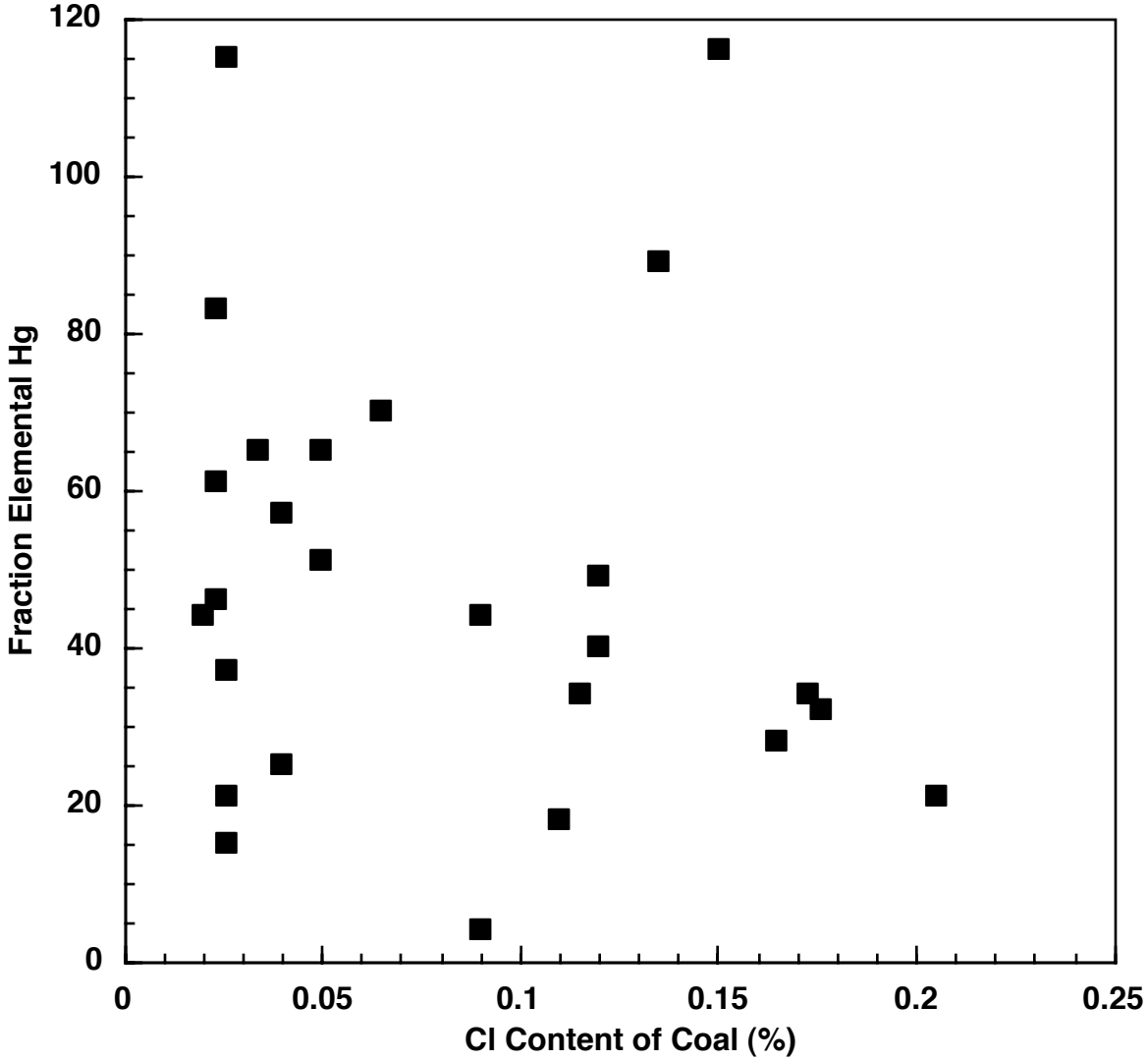

Figure 2.1. Influence of coal chlorine content on the oxidation state of mercury upstream of flue gas cleaning equipment.

Table 2.1. The Effect of Air Pollution Control Devices on Mercury Emissions (Jones, 1994)

Reduction in emissions, %	
Coal washing	30-40 %
Electrostatic Precipitators/fabric filter	0-60%
Flue Gas Desulphurization	10-90%
Total % of coal mercury emitted	5-95% emitted

2.4 Approaches for Controlling Mercury Emissions

Ideas for post-combustion mercury control have centered on existing air pollution control devices, or relatively simple modifications of these devices that improve their specific mercury performance. Much of this work was originally done to control toxic metals from municipal solid waste (MSW) incineration, and it is now being reevaluated for the lower metals content of coal. Flue gas desulfurization (FGD) devices have a wide range of mercury emission reduction. One example is the hydrated lime spray dryer for SO_2 control. The mercury removal of an unmodified spray dryer system is only 30-50%, but the addition of activated carbon in the flue gas leads to greater than 90% removal in some tests (Gleiser and Felsvant, 1994; Serre *et al.,* 2000); however, not all results have shown such high efficiency (Chow and Torrens, 1994). The use of iodine or sulfur impregnation on activated carbon leads to much higher captures of elemental mercury (Guijarro *et al.,* 1998; Mendioroz *et al.,* 1999; Hsu *et al.,* 2000), but leads to a higher cost sorbent. Zeolites have also been investigated as sorbents (Morency *et al.,* 2000), as have dry alkaline sorbents originally designed for SO_2 and HCl capture (Ghorishi and Gullett, 1998; Gullett *et al.,* 2000).

Wet scrubbers are relatively effective against oxidized mercury due to their low operating temperature (around 45° C), but still remove only 50-70% of elemental mercury (Meij, 1991). Only a few approaches for directly capturing elemental mercury have been proposed. For example, one proposal makes use of gold doping onto activated carbon to promote capture of mercury as an amalgam (Durham *et al.,* 1994). It has been more common to propose means of promoting oxidation since oxidized mercury is more effectively captured by existing equipment. Some advanced approaches to enhancing oxidation show promise, but remain the subject of uncertainty with respect to cost. One approach makes use of a pulsed corona discharge to promote mercury oxidation (Masuda, 1993). Widmer *et al.* (2000) estimated that this approach would require about 1% of a given power plant's electrical output. Another approach under consideration is the use of catalysts to promote oxidation ahead of wet FGD systems (Richardson *et al.,* 2000).

The very low concentration of mercury to be captured and the very large volume of flue gas that must be processed by the capturing equipment almost ensures that most control approaches will be very expensive when expressed on a cost per unit mercury captured basis. Cost estimates for mercury control range from $14,200-22,100 per pound of mercury removed (Environmental Protection Agency, 1997). Department of Energy estimates are higher. The technical uncertainties associated with mercury control, and the very high costs, are significant challenges should the power generation industry come under significant mercury regulation.

2.5 Mercury Oxidation Behavior

The amount of oxidized mercury measured in the field range widely depending (apparently) on fuel properties and combustor configuration. This suggests that oxidation may be controlled by relatively simple changes to the combustion process or by the use of chemical oxidation

promoters. As mentioned above, oxidized mercury is more easily captured by existing pollution control equipment. The goal is then a low-cost means of promoting oxidation that leads to enhanced capture in existing air pollution control equipment. This has motivated considerable work on understanding the fundamental processes that control oxidation and on developing novel concepts for promoting this reaction.

At combustion temperatures, equilibrium calculations show mercury will exist as elemental vapor. The kinetic rates are high enough at these temperatures that equilibrium probably represents a good model for behavior. Figure 2.2 shows equilibrium predictions for the speciation of mercury under specific temperatures and hydrochloric acid concentrations. These calculations included other mercury species and were performed against background concentrations of other gases that are typical of coal furnace flue gas (the HgO contribution to oxidized mercury is included with the $HgCl_2$ numbers). As can be seen in Figure 2.2, as the gases cool, the favored equilibrium product shifts to mercuric chloride ($HgCl_2$). The crossover temperature at which the favored equilibrium product shifts increases from 525°C to 640°C as the background hydrochloric acid goes from 50 to 500 ppm. This crossover point is not

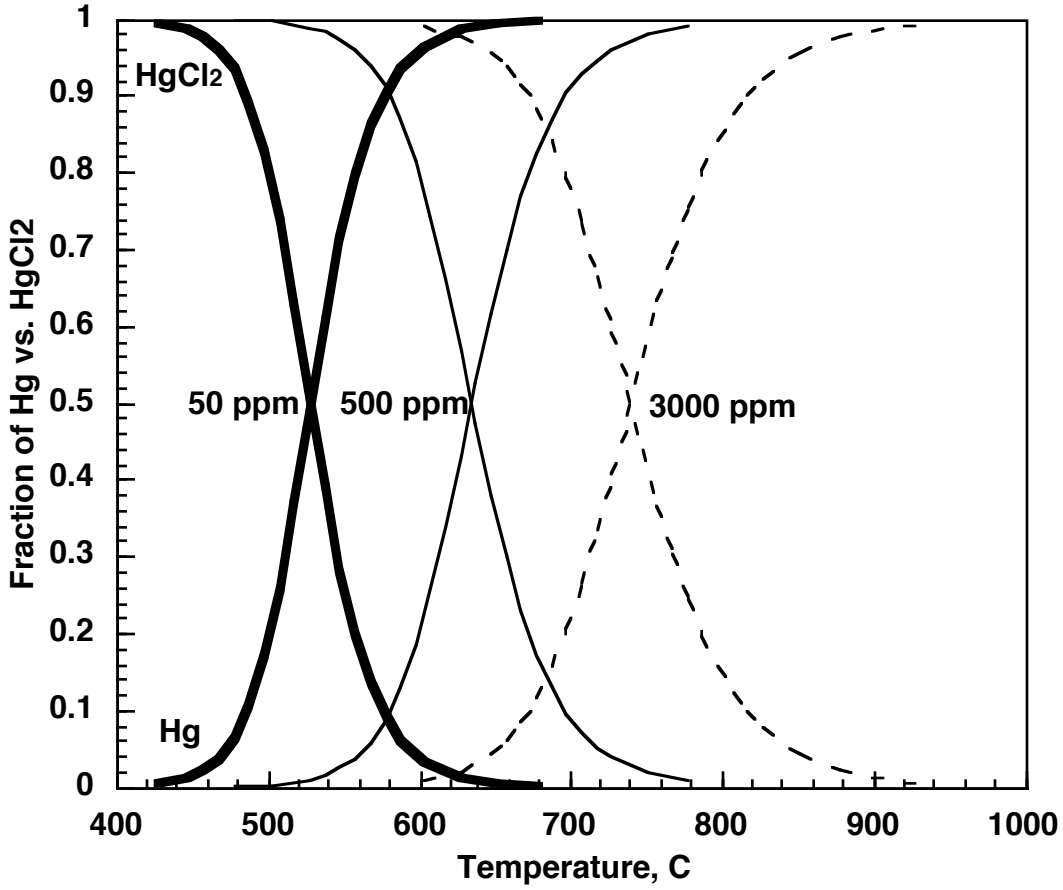

Figure 2.2. Equilibrium mercury oxidation behavior.

influenced by mercury concentration as long as hydrochloric acid is present in excess, which is the usual case. These trends are consistent with reports in the literature (Rizeq *et al*, 1994; Gullett, 1994).

Before discussing mercury oxidation kinetics, it is important to remember that chlorine will predominantly exist as HCl under these conditions. Depending on temperature, gas composition, quench rate, *etc.,* varying trace amounts of chlorine will be present as Cl, Cl_2, and other species.

Hall *et al.* (1990, 1991) performed flow reactor studies of mercury oxidation by a variety of species in flue gas and under an artificial background gas. These results show a fast reaction with Cl_2, even at room temperature. The oxidation with Cl_2 is much more complete in the artificial atmosphere relative to when water vapor and CO_2 are present, as is shown in Figure 2.3. Oxidation with HCl increases with temperature and HCl concentration, and is almost complete at the highest temperature studied (900°C), as shown in Figure 2.4. This is in marked contrast to the equilibrium calculations, which predict only elemental mercury at these high temperatures. The resolution of this apparent dilemma will be discussed later. Other experimental work (Widmer *et al.,* 1998; Lee *et al.,* 1998; Galbreath *et al.,* 1998; along with the present work discussed here) are consistent with the conclusion that mercury oxidation by HCl is favored by higher temperatures. These data, however, indicate that the extent of oxidation is reduced in flue gas as compared to a background gas that is free of CO_2 and water vapor. This is illustrated in Figure 2.5. The apparent much higher oxidation activity observed in the Hall experiments (for the same times and temperatures) relative to Widmer *et al.* and the present work will be discussed in Section 5.

Recent experiments by Mamani-Paco and Helble (2000) involve the injection of HCl into a mixing chamber that is immediately downstream of a flat flame burner that is seeded with mercury. The mixing chamber is followed by a non-isothermal flow reactor. While this experiment is similar to that of Widmer and the experiment reported herein, very little mercury oxidation is noted. The reason for this has not been resolved, but we will return to this issue in Section 5.0.

In summary, the data show that mercury can be globally oxidized by HCl and Cl_2 in homogeneous reactions. The reaction with HCl is of some interest since the majority of the chlorine released during combustion under fuel-lean conditions will appear as HCl. The almost complete oxidation observed at 900°C under the Hall *et al.* experiment is in contradiction to equilibrium. Also, the Hall data show much higher oxidation extents than data taken under typical flue gas environments for similar temperatures, mercury concentrations, HCl concentrations, and residence times. These issues will be addressed in Section 5.

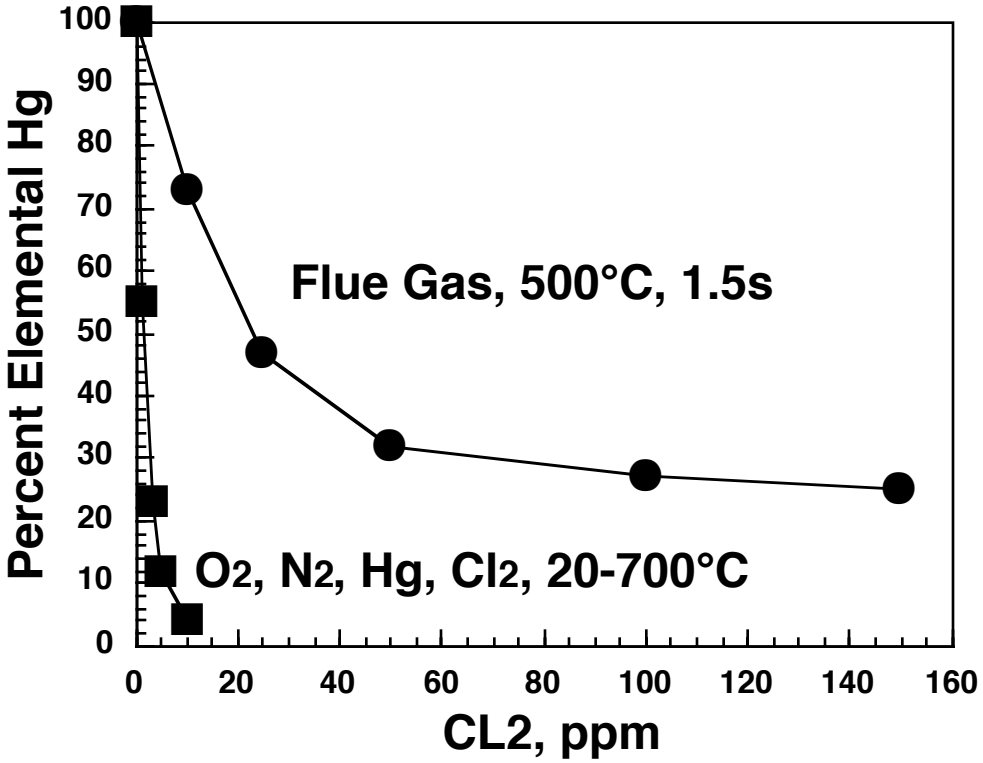

Figure 2.3. The influence of Cl_2 concentration on mercury oxidation (Hall *et al.,* 1991).

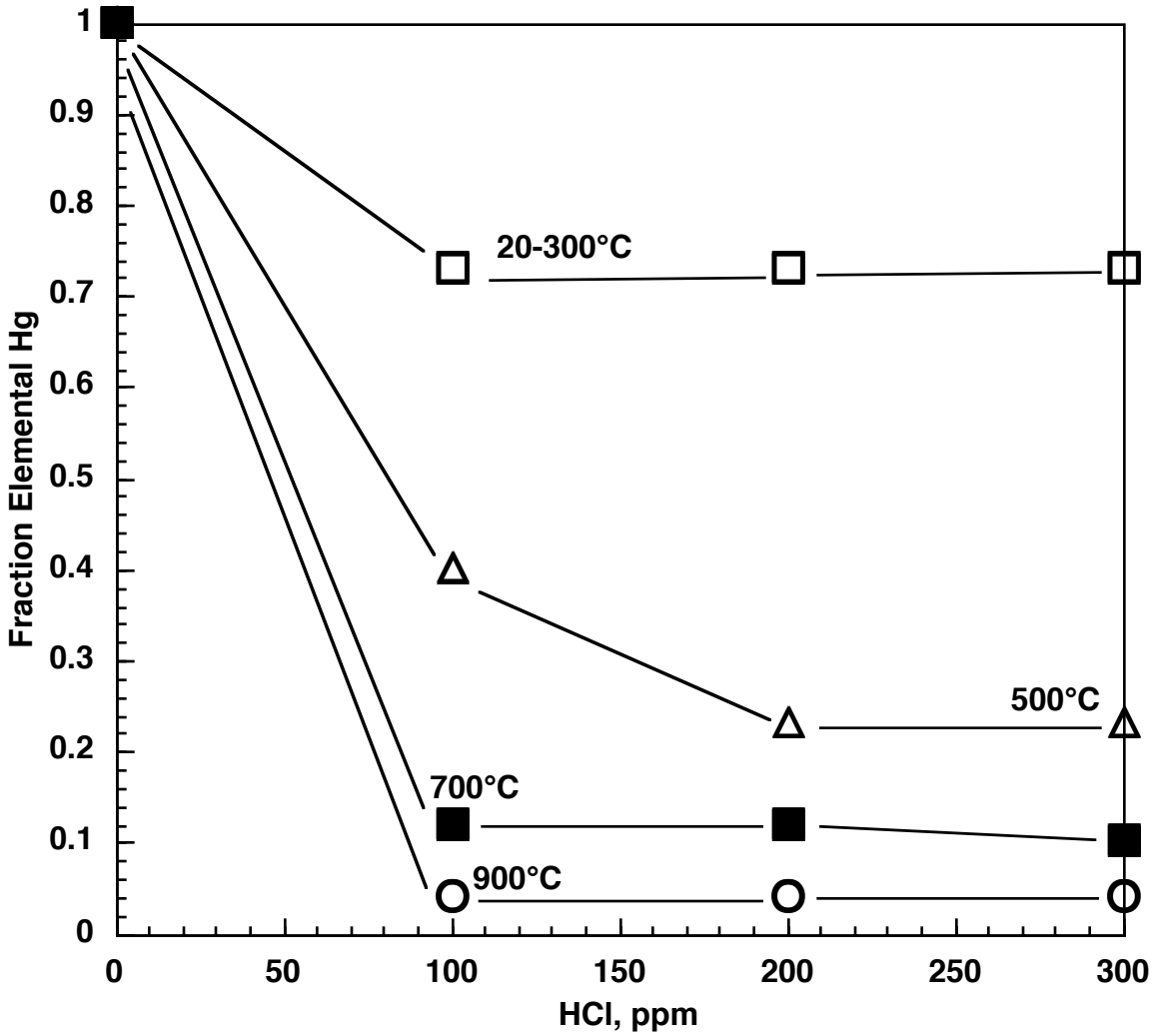

Figure 2.4. Data from Hall et al. (1991) showing the oxidation of mercury by HCl at various temperatures.

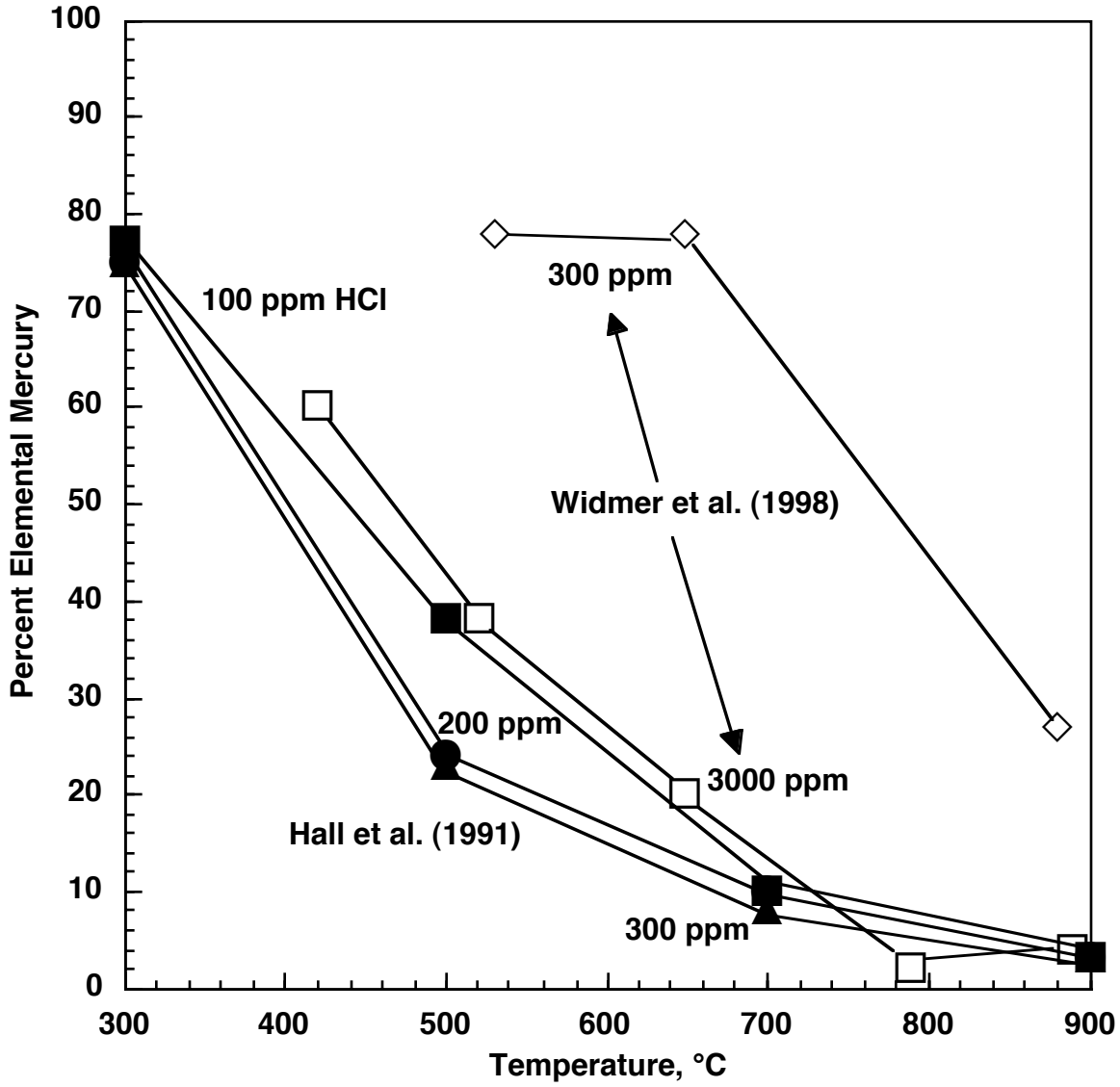

Figure 2.5. Comparison of mercury oxidation by HCl under flue gas environments (Widmer *et al*.) and under CO_2 and H_2O-free artificial atmospheres (Hall *et al*.).

2.6 Heterogeneous Mercury Behavior

At least three distinct ways have been suggested for heterogeneous behavior to influence the fate of mercury. These are:

- Interaction of mercury with coal ash.
- Capture of mercury by sorbents (discussed above).
- Promotion of catalytic Cl_2 generation followed by homogeneous mercury oxidation.

The intimate contact that occurs between coal ash and gaseous combustion products raises the issue of whether ash exerts a catalytic influence on oxidation. Early observations suggest that ash might catalytically promote oxidation (Laudal *et al.,* 1997; Karatza *et al.,* 1998). Testing on individual components in fly ash shows that Fe_2O_3 (Ghorishi *et al.,* 1999; Zhuang *et al.,* 2000) and CuO (Ghorishi *et al.,* 1999) can catalytically oxidize mercury in the presence of HCl. However, the presence of CaO tends to deactivate this process (Lee *et al.,* 2000). The powerful catalytic activity of CuO is suggested as one reason why mercury from waste incinerators (which typically contain much more copper in their ash) is so much more oxidized than that from coal combustion (Lee *et al.,* 2000). Some of the other major constituents in ash have been tested (TiO_2, SiO_2 and Al_2O_3) and found to not be active under HCl (Zhuang *et al.,* 2000; Lee *et al.,* 2000). Recent testing of coal ashes indicate little activity (Norton *et al.,* 2000). Thus, the implication is that while some components of coal ash can promote oxidation under HCl, mixed minerals tend to deactivate this effect.

Ash constituents have been found to promote catalytic oxidation under NO_2. Both SiO_2 and Al_2O_3 are active under these conditions (Ghorishi *et al.,* 1999). The NO_2 concentrations used in these studies (*e.g.,* 200 ppm) are, however, generally much higher than those found in practice.

The ability of activated carbon to absorb oxidized mercury is well known. Measurements have also shown that carbon in ash can absorb mercury (Hassett and Eylands, 1999). It has been suggested, however, that NO_2 can oxidize mercury off of carbon sorbents (Miller *et al.,* 1998). As mentioned above, a number of treatments for carbon surfaces have been investigated (iodine, sulfur, gold) as means of enhancing capture or promoting oxidation.

Another oxidation mechanism has been proposed by Senior *et al.* (1997). This is based on the homogeneous oxidation of mercury by Cl_2. Here, Cl_2 is catalytically generated by the interaction of HCl with fly ash and char. Once formed, the Cl_2 rapidly reacts with the Hg, and the oxidized mercury is partially captured by the char. This idea originates from mechanisms developed to explain the formation of chlorinated dibenzo-p-dioxins in downstream incineration equipment.

2.7 Status of Mercury Regulation

Although not directly relevant to the technical discussion at hand, the EPA's work towards developing a regulatory stance on mercury has been both a motivator for research in the field, and a mirror of the state-of-the-art. Thus, we briefly outline the present status of the regulatory efforts.

In 1990, the U. S. Congress passed the Clean Air Act Amendments, requiring that the Environmental Protection Agency evaluate emissions standards for 189 air toxins. Field evaluations by EPRI and DOE have shown that most toxic heavy metals recondense onto flyash in the post-flame region and are efficiently removed by existing fabric filters or electrostatic precipitators. Only mercury, selenium, and occasionally arsenic, escape with the flue gases. Of these, mercury is the greatest concern due to its high volatility.

In response to the 1990 Clean Air Act Amendments, the EPA prepared the "Mercury Study Report to Congress", released in December 1997. The report provides "an assessment of the magnitude of U. S. mercury emissions by source, the health and environmental implications of those emissions and the availability and cost of control technologies" (Environmental Protection Agency, 1997). The Mercury Report states that the U.S. emits approximately 159 tons of mercury per year from anthropogenic sources. The total annual global input to the atmosphere (from all natural and anthropogenic sources) is approximately 5500 tons. Therefore, U.S. anthropogenic sources contribute about 3% of total annual mercury input to the environment.

After considering the final report, the EPA Administrator concluded that additional information was needed (Cole *et al.,* 2000). To quote Cole *et al.*:

> "The EPA found that the available information, on balance, indicates that utility mercury emissions are of sufficient potential public health concern to merit further research and monitoring and acknowledged that there are substantial uncertainties that make it difficult to assess utility mercury emissions and controls. Among those uncertainties are the (1) actual cumulative mercury amount being emitted by all utility units, individually and collectively, on an annual basis' (2) speciation of the emitted mercury; and (3) effectiveness of various control technologies in reducing the volume of each form of mercury that is emitted."

These uncertainties have led the EPA to seek additional information. In particular, detailed inventories of the total mercury flow into each coal-fired power plant are being requested to develop a reliable value for the flow of mercury into the power generation process. At the same time, missed deadlines within the Clean Air Act Amendments has led to legal action, and the Agency is presently under court order to make a regulatory determination by 15 December 2000.

2.8 Implications

The community generally accepts the following conclusions regarding mercury:

- All of the mercury contained in coal is vaporized as elemental mercury during combustion. All conversions from this state come in the post-flame region.
- The presence of chlorine results in the appearance of oxidized mercury (Hg II) in the effluent.
- Mercury can be removed from the flue gases before the emission point. FGD equipment (especially wet scrubbers) are known to be effective at removing mercury, although the association of mercury with ash (or carbon in ash) also has the potential to contribute.
- Oxidized mercury is much more susceptible to removal than elemental mercury. This implies that promoting oxidation will promote mercury capture.

- Both homogeneous and heterogeneous processes are capable of influencing oxidation. The relative importance of the various potential pathways in practical combustion systems is, however, presently unclear.

Homogeneous oxidation has been demonstrated, but the actual chemical mechanism that causes it is undefined. One can postulate at least two reasons for identifying this mechanism:

- With the mechanism understood, it may be possible to identify means for promoting the oxidation.
- Any predictive model of mercury oxidation must contain an accurate homogeneous component, even if heterogeneous chemistry dominates.

Thus, the overall goal of this work is the identification and validation of an elementary homogeneous oxidation mechanism for mercury by chlorine species.

3.0 Experimental Apparatus and Procedures

3.1 Overview

Previous research in the area of mercury emissions has generally focused on actual coal combustion. When coal is burned, however, a large number of process which affect mercury emissions become active. This creates problems in trying to identify the fundamental processes governing the fate of mercury. Since the goal of this project is to focus on homogeneous mercury oxidation, a natural gas flame is used to provide the environment for the reaction. This eliminates heterogeneous reactions (except possibly those occurring on the walls of the furnace and sample system) and focuses on particular conditions of interest (*i.e.,* temperature, mercury concentration, and hydrochloric acid concentration). The flue gas is then sampled using a variation of EPA Emissions Test Method 29, "Determination of Metals Emissions from Stationary Sources". Although the Ontario Hydro method has become the more accepted wet chemistry approach to characterizing mercury emissions over the period of this grant, the SO_2 interference that is associated with Method 29 is not an issue here since the experiments are performed in a sulfur-free environment. Additional measurements make use of a Buck ultraviolet absorption analyzer for elemental mercury vapor.

3.2 Furnace Configuration

The natural gas furnace was designed and constructed in 1993 by University of Washington personnel to be used in coal and wood combustion experiments. Minor modifications were made to the furnace configuration in preparation for the mercury speciation experiments. Figure 3.1 shows a cross-section of the furnace, including the multiple layer refractory design, as it is presently used for high-temperature mercury testing.

The furnace is down-fired on natural gas and air with a maximum power rating of 16.1 kW (54900 BTU/hr). It stands 2.4 m (7.9 ft) tall, with the main burner sitting on top. As presently operated, the maximum flame temperature is 1600°C (2900°F). The furnace is equipped with ultraviolet flame detectors and other sensors to allow 24 hour operation. Around-the-clock operation is required because the refractory has such a high thermal inertia that the furnace takes several days to come to a steady state temperature. Since isothermal conditions are also preferable, four back-fired burners, forming two pairs of heating channels, are used along the middle section of the furnace. Although isothermal temperature conditions are not met due to the heat escaping the sides of the furnace, the backfire burners help minimize the temperature drop along the test section. Startup checklist procedures for the main and backfire burners are included in Appendix A. The sample ports, shown along the center of the furnace, allow for flue gas sampling. During testing, the second-to-lowest sampling port is used. This port allows for a long residence time, but, unlike the bottom port, the flue gas is still kept at a high temperature due to the backfire burners.

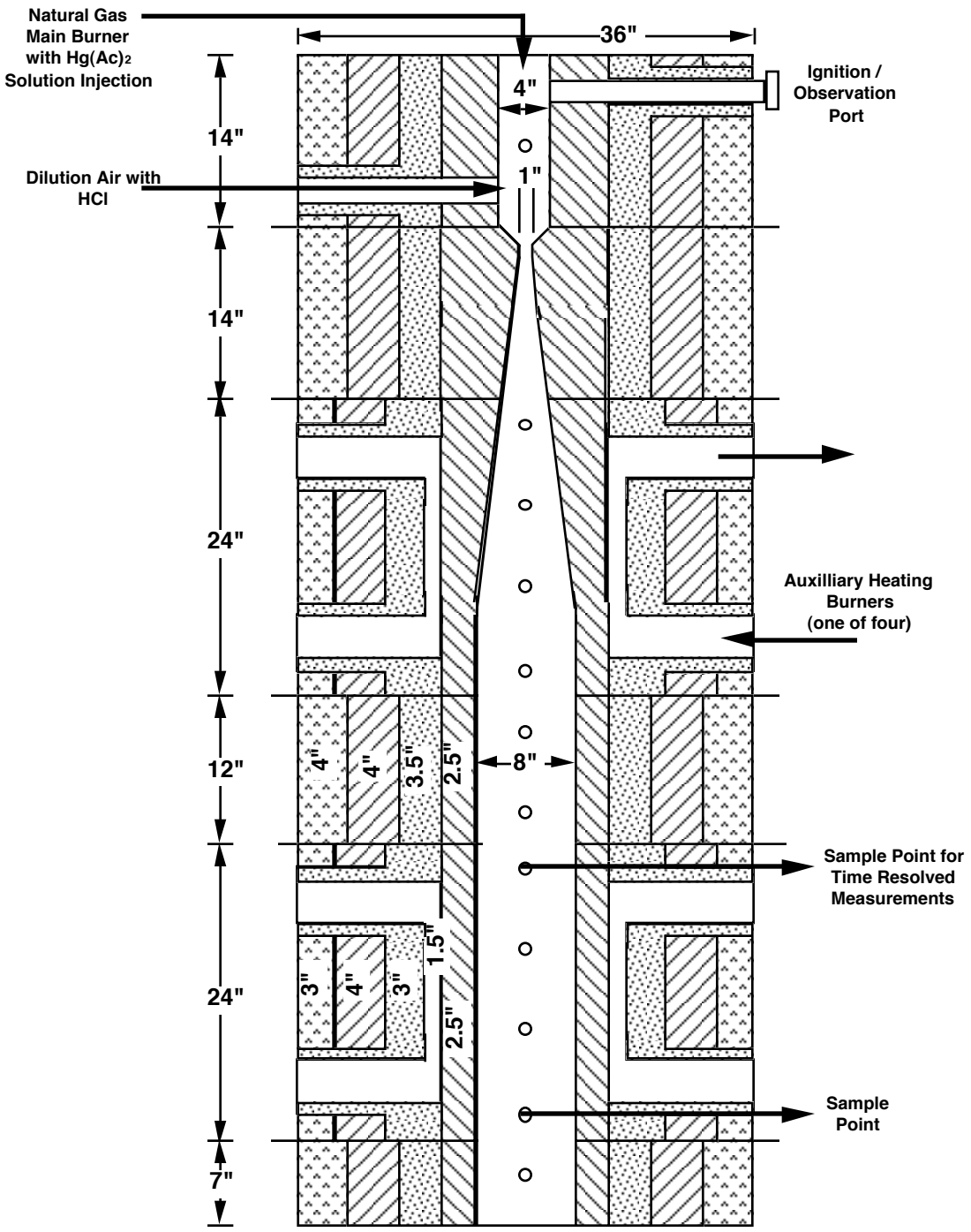

Figure 3.1 Cross-sectional diagram of the natural gas furnace.

During experiments, temperature measurements were taken using both a type K thermocouple (TC) and a high velocity thermocouple (HVTC). The TC has the advantage of providing a quick approximation of furnace temperature. This is particularly helpful since the furnace requires several days to reach steady state temperatures each time adjustments are made to the main burner or backfire burners. However, since the TC is affected by heat radiating to the cooler

interior wall of the furnace, the HVTC gives a more accurate temperature measurement. The HVTC draws the flue gas into a probe that is shielded by a thin tube of ceramic. The ceramic tube shields the thermocouple bead from optical access to the walls, and thus acts as a resistance to radiative heat transfer. In addition, the high-velocity flow of furnace gas over both the thermocouple and the shield provides a high convective loading, which increases the bead and shield temperature toward the gas temperature. Since the shield approaches the gas temperature, radiative loss from the bead is even further reduced. This allows the thermocouple in the HVTC to closely approximate the true gas temperature. Since the furnace walls are cooler than the flue gas, the HVTC temperature reading is generally 70-100 °C higher than the TC temperature reading. The disadvantage of using the HVTC is that it is more time consuming to set up. Therefore, the HVTC reading is only taken once the furnace has reached fairly stable conditions. Figure 3.2 shows the HVTC axial temperature profile for the nominal 922°C furnace condition. Here, the HCl is injected at 20 cm, and the sampling point is at 115 cm.

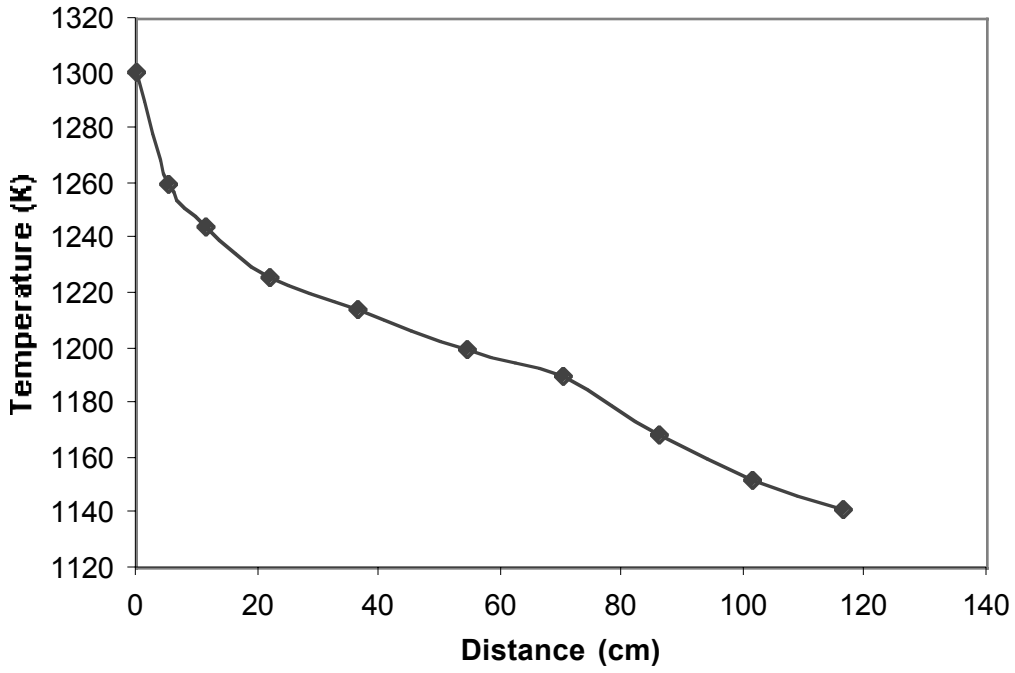

Figure 3.2. Furnace axial temperature profile.

As the gases enter the sampling train, they are exposed to a cold wall that quickly brings them to room temperature. Since the Reynolds number within the probe is less than 2300, the rate of cooling (after the start of the water cooling zone) can be approximately modeled as that of a fully-developed laminar flow encountering a step change in wall temperature. (Note that this assumes all the resistance to heat transfer lies in the gas film. This is appropriate given the high thermal conductivity associated with the quartz wall and the cooling water that surrounds the quench region of the probe.) The results of such a calculation are shown in Figure 3.3. This indicates a quench rate of the order of 5400 K/s. As we shall see in Section 5, the chemical kinetic model suggests that reactions occurring during this quench are important to the overall

oxidation. Thus, the probe and quench region should be viewed as extensions to the reaction zone of the high temperature furnace, and the modeling of their thermal history is important.

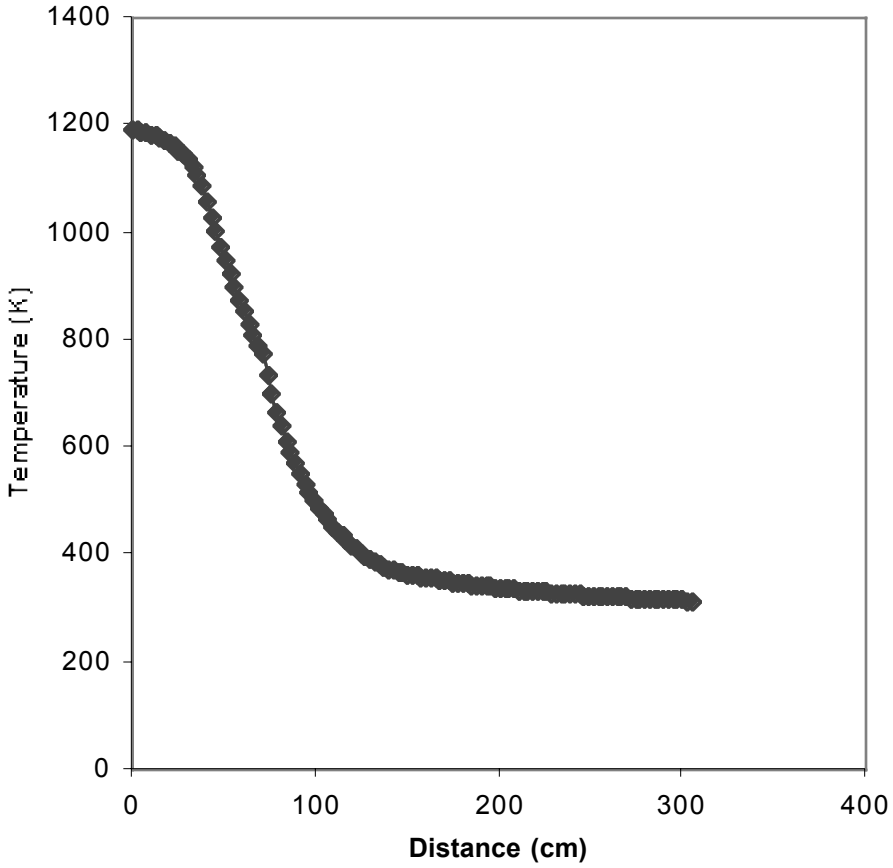

Figure 3.3. Temperature history of the gases within the sampling system (referenced to the probe inlet).

During testing, a mercuric acetate or mercury nitrate solution is atomized into the primary flame. The high temperature of the flame ensures that the acetate or nitrate is decomposed and the mercury is reduced to elemental mercury. This point has been verified by injecting mercury in the absence of hydrochloric acid; measurements show the entire recovery to be elemental rather than oxidized mercury. Initial testing showed an unacceptable variability in the mercury injection rate. This was traced to precipitation of mercury from the injection solution, effectively leading to mercury concentration gradients in the solution. This was controlled by acidifing the solution with nitric acid. This prevented precipitation and provided a uniform concentration within the feed solution (see Section 3.6 for a detailed discussion).

A lance is used to inject cooling air at the throat of the venturi as shown on the figure. Variations in the stoichiometry of the main burner and cooling air injection bring the gases to the desired temperature in the test section. The hydrochloric acid is doped into the dilution air, so the region

between the air injection point and the sample probe inlet corresponds to the test section. Temperature profiles through the furnace have been measured with a suction pyrometer, and conditions for isothermal operation identified. For all cases with variable dilution air addition, the residence time is approximately 1.4 seconds. The residence time stays nearly constant because the additional mass flow associated with the higher cooling air flow is offset by the higher density associated with the cooler temperature. Flue gas samples were taken using a modified version of EPA Method 29 or via the Buck ultraviolet analyzer.

3.3 EPA Method 29

In order to determine the fraction of mercury in the flue gas which was oxidized, an effective means of differentiating between the species is required. Method 29 is an EPA method used to evaluate the total concentration of various trace metals. Although Method 29 is a recognized method for detecting total mercury concentrations, there is still some debate about its ability to distinguish between elemental and oxidized mercury. The primary concern is that the presence of sulfur dioxide (SO_2) and molecular chlorine (Cl_2) can cause elemental mercury to be measured as oxidized mercury. (Chu *et al.*, 1995, EERC, 1996, Krivanek, 1996). However, sulfur dioxide is not present in the experiments. In all tests performed to date, molecular chlorine is present, but at concentrations less than one part per billion. Studies indicate a possible interference problem at levels greater than fifty parts per million (Linak, 1998). For the initial tests, Method 29 appeared to be a satisfactory method for mercury speciation.

In Method 29, the sample is extracted from the duct using a quartz-lined probe. Since no particles are present, the usual filter is omitted. The flue gas passes through a series of impingers; the first set contains nitric acid/hydrogen peroxide followed by a another set with acidified potassium permanganate. The nitric acid impingers collect the various forms of oxidized mercury, but do not collect the elemental form. The permanganate impingers oxidize the elemental mercury and retain it in solution in oxidized form. Before the gas reaches the nitric acid and permangante impingers, it passes through an optional empty knockout impinger which collects excess moisture during the 240 minute runtime. This long sampling period is suggested by Method 29 to provide higher mercury concentration sensitivity. Mercury concentration is analyzed by CVAAS at a local lab. Checklists for performing runs and preparing samples are included in Appendix B.

The primary disadvantage with Method 29 is that it is a time consuming process. Although CVAAS is performed off-site, chemical preparation, setup, sampling and sample preparation time limit experiments to one or two tests per week. Once samples are sent to the off-site lab, results generally take three to four weeks to be reported. Since almost a month may pass between when a test is performed and its results are received, it is difficult to use results to modify a test series while it is in progress. Since wet chemical methods are the currently accepted procedures for mercury speciation, experimental research in this field is slow and tedious for all researchers. This has been a principal reason for the slow progress in developing an understanding of the factors that govern mercury behavior.

3.4 Cold Vapor Atomic Adsorption Spectroscopy

In the CVAAS process, an aliquot of each of the mercury catch fractions (*i.e*., the nitric acid impingers or the permanganate impingers) is individually analyzed. A stannous chloride ($SnCl_2$) solution is added to each catch fraction, which reduces the oxidized mercury in solution to elemental mercury. Since the elemental form is essentially insoluble in the solution, the mercury is released as a vapor. A purge stream entrains the vapor and passes it through an optical cell tuned to 253 nm. The integral of the absorption signal with time provides a measure of the total amount of mercury released from the aliquot under consideration. A simple calibration is used to generate quantitative information from the raw signal (Method 303F).

Initially, CVAAS was performed at the University of Washington Medical Center Laboratory. The Medical Laboratory's procedure is designed to analyze urine and blood samples. The disadvantages of using the Medical Lab for CVAAS are:

1. The inability to detect mercury levels below the 5 ng/ml,
2. All sample preparation prior to CVAAS analysis must be performed in the combustion lab, a time consuming process.
3. The Medical Laboratory only runs mercury tests once a week. The day and time when the procedure is performed vary according to demand and work load. In one step of chemical preparation performed by the combustion lab, the contents of the $KMnO_4/H_2SO_4$ impingers are filtered. The filter itself is digested and becomes another sample. However, since CVAAS must be performed on the filtrate within 48 hours, samples for a single test run were tested a week apart. Method 29's time constraint and the Medical Lab's varying schedule made sample coordination challenging.
4. The Medical Lab's test is not designed for high concentration solutions. During testing, mercury is injected into the furnace using a syringe drive containing a high mercury concentration solution. Quantitative measurements of the mercury concentration in the syringe are used to predict the mercury concentration in the flue gas. Since, the concentration of the syringe samples were significantly higher than the maximum level of the Medical Laboratory's test, technicians were concerned about performing these tests.

After several tests were performed by the Medical Laboratory, a local company was found which performs EPA tests such as Method 29. AmTest Inc. is able to perform not only the CVAAS section of Method 29, but also some of the sample preparation. Our laboratory provides AmTest with the contents of the impingers (and the solutions used to rinse the impingers) after a test run has been completed. AmTest then prepares the samples and performs the CVAAS. The advantages of using AmTest are:

- Improved detection levels to 0.1 ng/ml.
- Significantly less analytical time in the combustion lab, increasing the number of tests that can be performed,

- Since all filtering steps are done at Am Test, the 48 hour time constraint is no longer an issue,
- The mercury concentration in the syringe is tested.

The difference in procedure between using the University of Washington Medical Laboratory and AmTest for CVAAS can be seen in the post-run checklists included in Appendix B.

3.5 Ultraviolet Analysis

An alternate measurement strategy makes use of a Buck elemental mercury analyzer. This analyzer characterizes elemental mercury via UV absorption on an extracted sample. In the present experiments, the HCl flow can be switched on and off at will and the change in the elemental mercury signal can be taken as indicating the amount of oxidized mercury produced. A test under a very high HCl flow shows essentially a zero signal, indicating that oxidized mercury does not interfere with the elemental reading. For this measurement approach, the same probe and sample quench systems were used as with Method 29. An impinger was used to remove water and dry the sample down to a 0°C dewpoint. As discussed later, this method yielded consistent results with Method 29, but with a large reduction in the amount of time needed to obtain an analysis. A checklist for the operation of this method is included in Appendix B.

3.6 Experimental Challenges

One of the most challenging aspects of these experiments is accurate mercury injection into the furnace. As stated above, the syringe concentrations are selected in order to provide a furnace concentration of about 53 $\mu g/m^3$. A large batch of mercury solution was made, and a sample of the syringe solution was sent to AmTest or the UW Medical Laboratory along with the test samples. However, laboratory testing of the syringe samples shows significant variation from one syringe sample to another.

The inconsistency in mercury concentration is attributed to the tendency of the mercury solution to precipitate during storage and prior to injection. This tendency has also been noted by other researchers (Linak, 1998). Samples of the syringe solution sent to be analyzed only contain water soluble mercury. During experiments, both the soluble mercury and the mercury-containing precipitate would be injected. Therefore, the "expected" concentration is probably a more accurate reflection of the amount injected into the furnace. Acidifying the injector solution with HNO_3 will prevent mercury precipitation (Linak, 1998). The difficulty in identifying precise mercury concentration in the flue gas is not as significant as it first appears, however, because the oxidation behavior is not strongly influenced by mercury concentration (see Section 4). This relative insensitivity of oxidation to mercury concentration allowed us to select a higher mercury concentration, and enhance mercury detection.

A second significant experimental challenge is the time required to perform Method 29. This time-consuming process limits the amount of data collected. This was a principal reason for

moving to the ultraviolet analyzer. Buck Scientific, Inc. makes a mercury analyzer which converts all the mercury to elemental mercury (per EPA Method 245.1) and then measures the total elemental mercury concentration. Since this research is specifically focused on oxidation, a method which immediately reduces all the mercury to its elemental form does not seem applicable. However, the reduction step can be bypassed, making the instrument sensitive only to elemental mercury.

4.0 Experimental Results

4.1 Overview

The principal variables examined in the present experiments are (1) HCl concentration, (2) furnace temperature, and (3) initial mercury concentration. These results are compared with those from the literature for consistency and differences. Section 5 discusses the development and application of a chemical kinetic model for these data.

4.2 Experimental Tests

The initial test series made use of Method 29. The nominal mercury injection rate produces a mercury concentration of 53 $\mu g/Nm^3$, which is towards the high end of the range encountered in coal combustion practice (Brown *et al.,* 1999). This higher mercury concentration improved the sensitivity of the analytical technique. For the test performed at 860°C a concentration of 137 $\mu g/Nm^3$ is used.

The baseline composition of the post-flame gas for the 922°C reactor is as follows:

O_2	7.43%
CO_2	6.15%
H_2O	12.3%
NO_x	25 ppm
Hg°	53 $\mu g/m^3$
HCl	varied as indicated
N_2	balance

The concentrations are similar for the other reactor temperatures.

Prior to starting the mercury oxidation experiments, a test run was performed in which neither mercury acetate nor hydrochloric acid was injected. As expected, the results of this test showed no detectable mercury in the furnace flue gas. Table 4.1 lists the results of all the data from this initial test series. Three runs are not included in the table, since problems with the syringe drive (two tests) or use of the wrong mercury concentration in the syringe (one test) made the results invalid. Test runs were performed for three furnace temperatures, which are shown in Table 4.1. Complete data sets for each of the tests are included in Appendix C. Note that in the absence of HCl, essentially no mercury oxidation occurs. As noted above, the mercury injection solution had to be acidified to prevent mercury precipitation, which otherwise leads to unacceptable variations in mercury inlet flow rates. With this done, the recoveries were typically in the 80-120% of expected range using Method 29.

Table 4.1 Percent Oxidized Mercury Based on Experimental Results

Approximate Sample Temp (C)	HCl (ppm)	% oxidized mercury	date	actual sample temp (C)
922	56	0	5/12/97	918
	172	33	5/23/97	930
	175	27	4/24/97	929
	282	41	4/11/97	917
	453	29	4/24/97	929
860	0	0	4/7/97	868
	0	2	6/5/97	853
	131	11	6/11/97	858
1071	0	0	7/29/97	1071
	638	75	8/4/97	1071

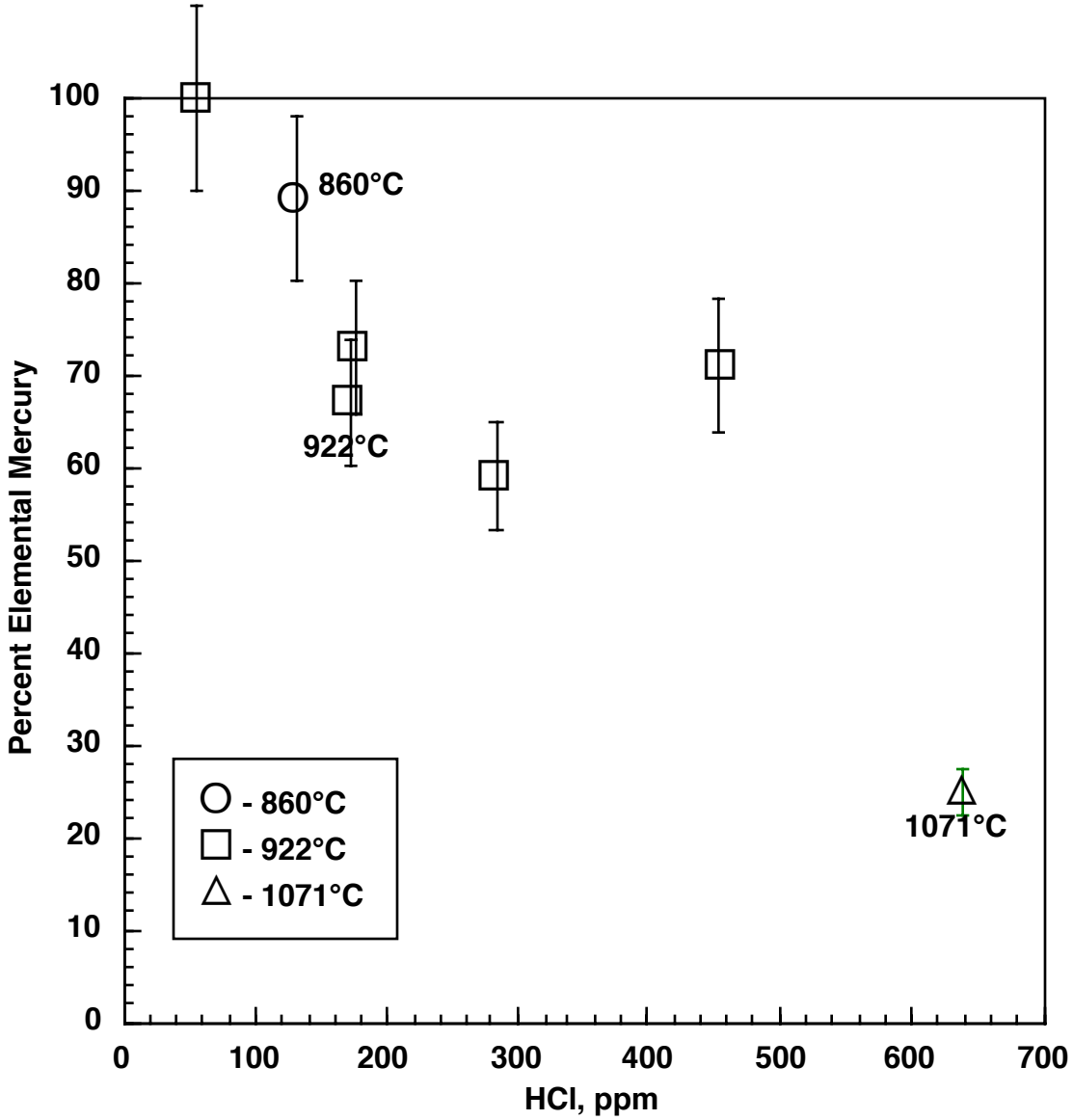

Figure 4.1 Mercury oxidation as a function of HCl concentration and temperature.

Figure 4.1 shows the data graphically, along with the error bars estimated from an uncertainty analysis performed on each of the component measurements that go into the overall reported value for mercury oxidation. No clear trend with temperature is noted.

Figure 4.2 compares the present data with the literature for similar experimental temperatures. Although the present experiment uses a longer reaction time, the extent of oxidation is less than the literature experiments. The significantly higher mercury concentrations used in the Widmer experiments might be expected to lead to less oxidation, but here more oxidation is observed. One clear difference is the fact that simulated flue gases are used in the present data and in Widmer, while only O_2, HCl, Hg and inerts were present in the Hall experiments. This difference will be explored via chemical kinetic modeling in Section 5.

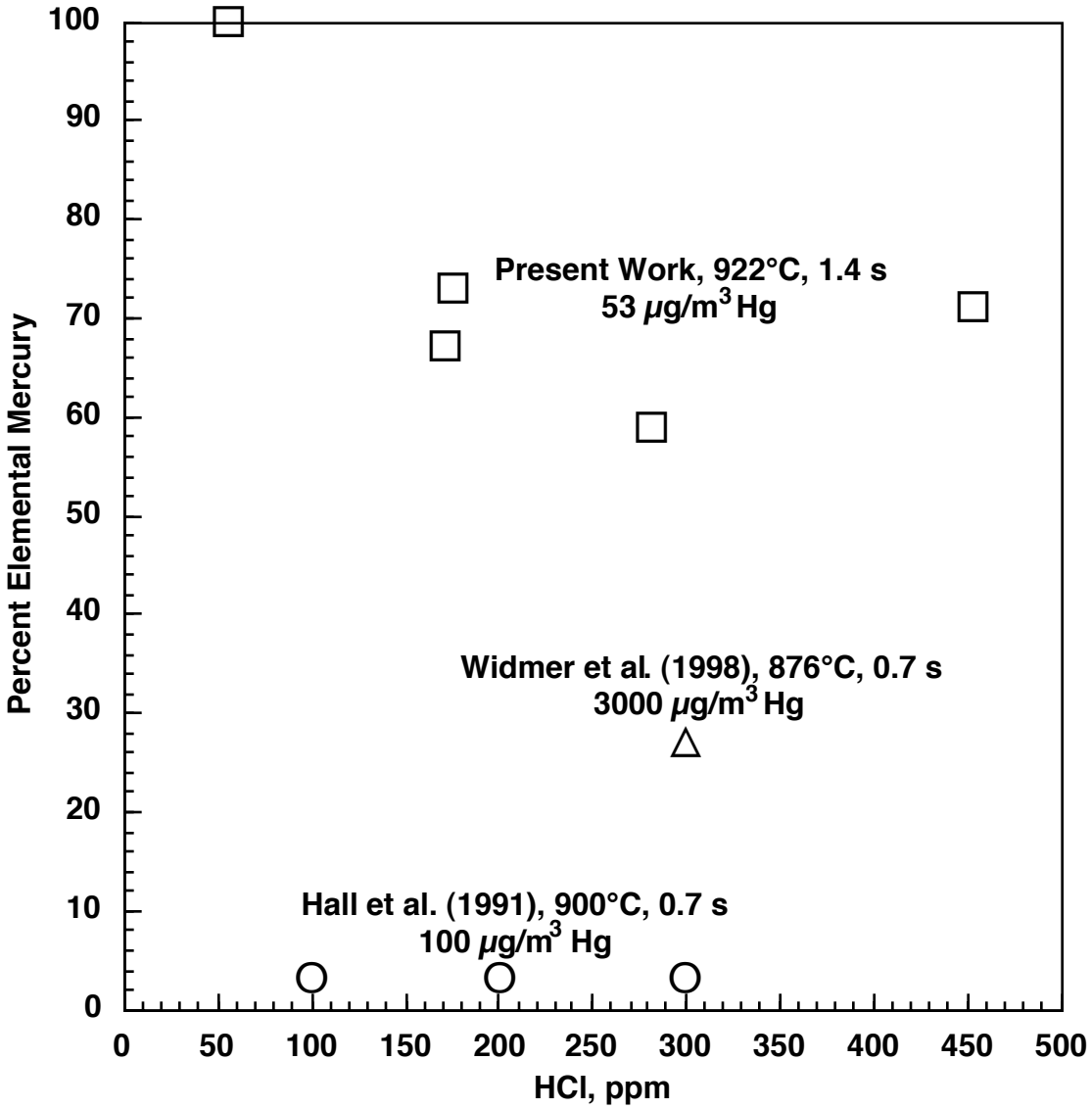

Figure 4.2. Comparison of the present data with literature data for similar temperatures and residence times.

Figure 4.3 compares data taken at various initial mercury concentrations at 922°C. This includes data obtained with both Method 29 (those data at 53 μg/Nm^3 initial mercury concentration) and with the ultraviolet analyzer (the remaining data). (All of these data are presented in tabular form in Appendix C.) Within the scatter, no clear trend is seen between mercury concentration and fractional oxidation. Note that there is apparent consistency between the wet chemical technique and the analyzer. A multiple linear regression analysis on the influence of both the HCl concentration and the mercury concentration on fractional oxidation yields the following correlation coefficients (See Appendix C for details):

$$r^2(\text{HCl vs. \%ox}) = 0.76$$
$$r^2(\text{Hg vs. \%ox}) = 0.07$$

Thus, there appears to be little evidence for a correlation between the initial mercury concentration and the fraction that is oxidized, even though a range of over 25x in initial mercury concentration was examined.

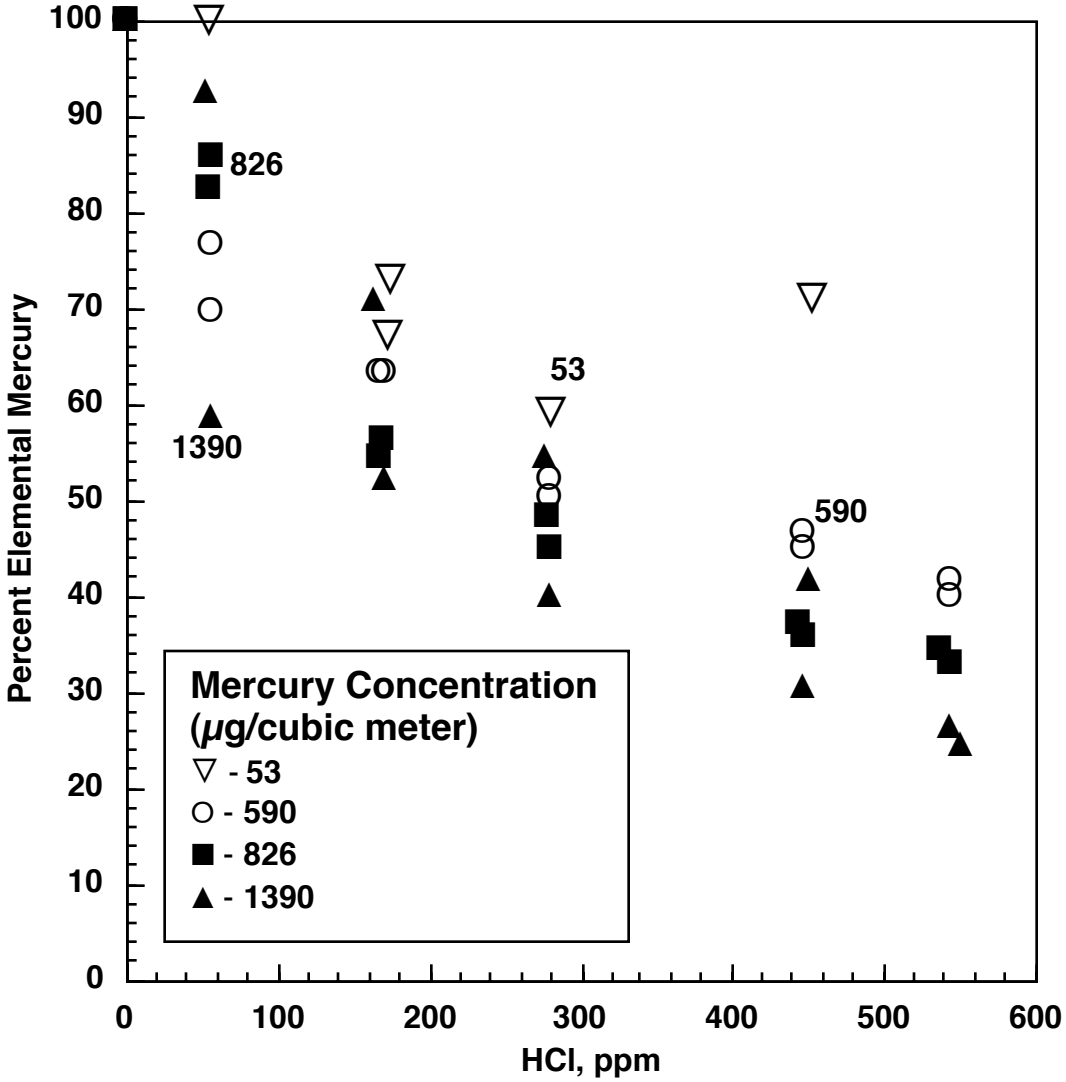

Figure 4.3. Mercury oxidation data at various initial mercury concentrations.

In summary, the general observations from our experimental work are as follows:

- Under our experimental conditions, no mercury oxidation is observed in the absence of chlorine.
- Increased chlorine always leads to increased oxidation. The asymptotic oxidation yields at high HCl levels observed in the Hall *et al.* data are not observed in our experiments. We did not, however, operate at the lower temperatures where Hall observed this feature.
- Our oxidation extents are less than those of Hall *et al.* Other data in flue gas environments also shows less oxidation that that of Hall, who performed their experiments in an artificial atmosphere that was free of CO_2 and water vapor.
- Our data do not indicate any statistically significant correlation between oxidation extent and initial mercury concentration.
- Under the present conditions, temperature did not significantly influence mercury oxidation.

5.0 Chemical Kinetic Mechanism Development

Experiments have clearly demonstrated that homogeneous oxidation of mercury can occur. Both HCl and Cl_2 have been shown to be active in promoting global oxidation. Calculations using global rate constants derived from the data of Hall *et al.* (1991) have been performed (Senior *et al.,* 2000). Our approach will be to attempt to address the problem through elementary reactions.

The elementary reaction of Hg with HCl is a reaction that must be considered since HCl is the predominant chlorine species under practical flame and post-flame conditions. The direct reaction:

$$Hg + HCl \rightarrow HgCl + H \qquad (5.1)$$

is unlikely to be important, however. It is a strongly endothermic reaction with a high energy barrier (Hranisavljevic and Fontijn, 1997). Widmer *et al.* (2000) estimate a rate constant via a collision-limit preexponential term and an activation energy equivalent to the Δh for the reaction:

$$k_{5.1} = 4.94E+14 \bullet \exp(-39{,}910/T)$$

This results in an insignificant rate under all relevant conditions. Thus, the elementary oxidation reactions must involve other species that are derived from HCl.

The observation that the global oxidation of mercury by HCl is promoted by high temperature suggests that the key species may be reactive free radicals or other species that are derived from HCl. The concentration of such a radical would be expected to be strongly dependent on temperature. One likely candidate is atomic chlorine.

The fast oxidation of mercury at room temperature via:

$$Hg + Cl \rightarrow HgCl \qquad (5.2)$$

has been reported in the literature with $k_{5.2}=1.95\pm1.05\text{x}10^{13}$ cm^3/mole-s (Horne *et al.,* 1968). The rate constant is within an order of magnitude of the collisional limit, which is not unexpected for such an exothermic free radical reaction. Widmer *et al.* (2000) derive a rate expression for this reaction by using mechanistic estimates for other reactions in the mercury/chlorine system and then adjusting the Arrhenius parameters for Reaction 5.2 until they matched their data. This results in a rate constant about 15 times higher than the Horne *et al.* result. Although the uncertainty associated with basing this rate constant on estimates of the other rate constants in the mercury/chlorine system must be considered, the results do suggest a fast reaction. The key problem is then obtaining an accurate estimate for Cl-atom behavior.

A second oxidation reaction is with Cl_2. The direct, room temperature oxidation of mercury by Cl_2 was observed by Hall *et al.* (1991). The results were obtained by varying the Cl_2 concentration and observing the extent of oxidation at the exit. The conversion was independent of temperature between 20 and 700°C, and was essentially complete when the Cl_2 concentration reached 10 ppm (see Figure 2.3). These data can be analyzed to generate a second order global rate constant:

$$Hg + Cl_2 \rightarrow \text{oxidized products } (HgCl_2?) \tag{5.3}$$

with $k_{5.3}=3.4x10^9$ (cm^3/mole-s) A similar experiment was performed at 500°C using flue gas as the background for the reaction. In this case, the extent of oxidation was substantially reduced (*e.g.*, to only 25% at 10 ppm Cl_2, also shown in Figure 2.3). This suggests the presence of the flue gas constituents (*e.g.*, CO_2, H_2O, O_2) interfere in this mercury oxidation process.

Widmer *et al.* (2000) feel that the rate for the elementary reaction is much slower than indicated by this global rate constant. They suggest that the elementary reaction sequence is:

$$Hg + Cl_2 \rightarrow HgCl + Cl \tag{5.4}$$

which leads to chlorine atoms that can quickly react via Reaction 5.2. Thus, the implied chain branching will lead to a global oxidation rate that will substantially exceed the elementary reaction rate. At high temperatures, however, Cl_2 is not a favored species, and it appears only as the gases quench towards room temperature. As we shall shortly see, Cl_2 may indeed play a role at lower temperature.

The subsequent oxidation of HgCl to $HgCl_2$ could occur via several paths, including:

$$HgCl + HCl \rightarrow HgCl_2 + H \tag{5.5}$$
$$HgCl + Cl_2 \rightarrow HgCl_2 + Cl \tag{5.6}$$
$$HgCl + Cl \rightarrow HgCl_2 \tag{5.7}$$

Although an abstraction path must be considered for the latter reaction:

$$HgCl + Cl \rightarrow Hg + Cl_2 \tag{5.8}$$

Due to the high concentration of HCl in the system, Reaction 5.5 was initially considered a likely candidate. It has been considered in some detail.

The geometries of the reactants and transition state for the $HgCl_2+H \rightarrow HgCl+HCl$ ($k_{5.5b}$) reaction were determined using the B3LYP hybrid density functional theory (Becke, 1988, 1993; Lee *et al.,* 1988) with a standard double-zeta basis set, LANL2DZ, associated with the relativistic effective core potential (ECP) for mercury (Wadt and Hay, 1985), and the nonrelativistic ECP for chlorine. The optimized geometries of the reactants and transition state

for this reaction are shown in Figure 5.1. The relative energy, zero-point vibrational energy correction, rotational constants, and frequencies obtained at the B3LYP//LANL2DZ level of theory using Gaussian98 (Frisch *et al.,* 1998) are shown in Table 5.1. We have assumed that the reaction of $HgCl_2$ with H-atom occurs by direct chlorine abstraction, produces HgCl+HCl without involving a long-lived complex, and has two equivalent reaction pathways leading to products. The transition state was determined to be nearly linear and is shown as TS1 in Figure 5.1. The critical energy barrier for this reaction lies slightly downhill from the $HgCl_2$ and H

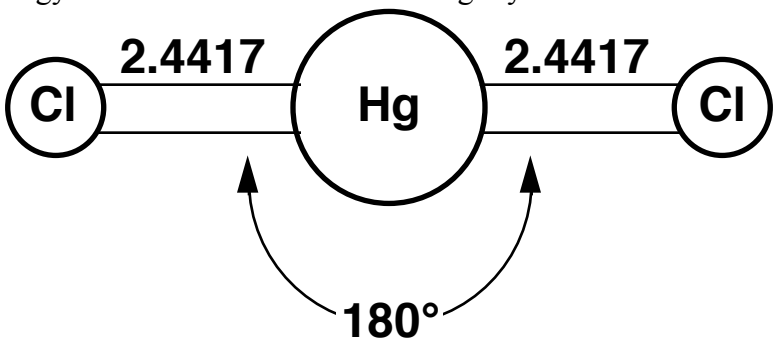

1. $HgCl_2$

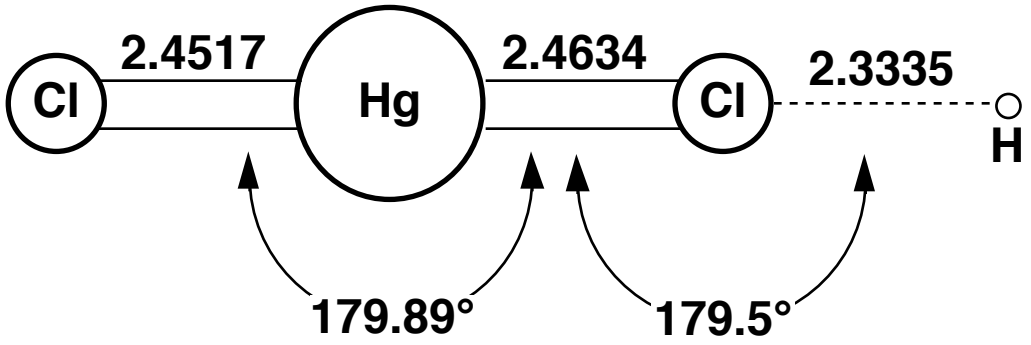

2. TS1

Figure 5.1. Optimized geometries of $HgCl_2$ and the H···Cl···Hg-Cl transition state involved in the $HgCl_2$+H reaction at the B3LYP/LANL2DZ level of theory. Bond lengths and bond angles are in units of angstrom and degree.

reactants by approximately -0.19 kcal/mol. Conventional transition-state theory was employed to calculate the rate constant for the $HgCl_2$+H → HgCl+HCl reaction. The calculation was based on the critical energy computed using the B3LYP hybrid density functional method. According to the general TST, rate constant k at temperature T for a bimolecular reaction can be expressed as (Conners, 1990; Steinfeld *et al.,* 1999)

$$k(T) = L^{\ddagger} k_B T/h \exp(-\Delta G^{\ddagger}(T)/k_B T)$$

The $L^{\ddagger}$ is the statistical factor which accounts for the number of equivalent reaction pathways; h is the Planck's constant; k_B is Boltzmann constant; and $\Delta G^{\ddagger}(T)$ is the standard-state free energy of activation change at temperature, T, going from the initial state to the transition state. A least squares analysis of the calculated rate constants leads to the following rate expression:

Table 5.1
Relative Energies, Zero-Point Energy Correction, Rotational Constants, and Frequencies of Reactants and Transition State

Species	Relative Energy (in Hartrees)	Zero-Point Energy Correction (in Hartrees)	Rotational Constants (cm^{-1})	Frequencies[a] (cm^{-1})
H···Cl··Hg-Cl	-73.2150355	0.001986	22200.26 0.03782 0.03782	61,90, 103,283, 335,247i[b]
Cl-Hg-Cl	-72.7158256	0.000521	0.0 0.03782 0.03782	66,66 288,345
H	-0.4989111	–	–	–

(a) Frequencies are not scaled
(b) Denotes the imaginary frequency

$$k_{5.5b} = 6.406E{+}09\ T^{1.02} \exp(+195K/T)\quad cm^3/mole\text{-}sec$$

valid over the 900-2000 K temperature range. The rate constant for the reverse reaction may be obtained through the principle of detailed balancing. The $HgCl_2+H \leftrightarrow HgCl+HCl$ equilibrium constant was calculated as $K_{eq} = 1.381E{+}06\ T^{-1.48} \exp(9811/T)$ from the JANAF Tables (Chase *et al.,* 1985). The $HgCl+HCl \rightarrow HgCl_2+H$ rate expression was determined from $K_{eq}=k_{5.5b}/k_{5.5f}$ and the following result was obtained

$$k_{5.5} = 4.638E{+}03\ T^{2.5} \exp(-9616K/T)\quad cm^3/mole\text{-}sec$$

for the 900-2000K temperature range. The estimated error on this rate constant is plus or minus a factor of four. This reaction is thus very slow under the present conditions, and as will be seen presently, does not significantly contribute to oxidation.

Rate data for Reaction 5.6 are not available. Widmer *et al.* (2000) have estimated a rate constant based on a preexponential factor that matches the $Hg + Cl_2$ reaction and an activation energy that is consistent with that of similar species. This results in the expression:

$$k_{5.6}=1.39E+14 \exp(-503/T)$$

which is essentially at the collision limit. Likewise, Reaction 5.7 is also likely to proceed near the collision limit. No data or estimates are available for the abstraction branching ratio of the HgCl+Cl reaction.

Widmer *et al.* (2000) also hypothesize two additional reactions via HOCl:

$$Hg + HOCl \rightarrow HgCl + OH \quad (5.9)$$

$$HgCl + HOCl \rightarrow HgCl_2 + OH \quad (5.10)$$

Reaction 5.9 is hypothesized to have a large activation energy and would likely not compete. Reaction 5.10 is estimated to proceed near the collsional limit.

This review of the likely means of interaction between mercury and chlorine results is a surprisingly simple picture with only a limited number of uncertainties. One elementary reaction that can clearly oxidized mercury is:

$$Hg + Cl \rightarrow HgCl \quad (5.2)$$

which proceeds near the collisional limit. The elementary reaction:

$$Hg + Cl_2 \rightarrow HgCl + Cl \quad (5.4)$$

is slower, and suffers from an absence of Cl_2 at high temperatures. However, its chain-branching character may accelerate its importance at lower temperatures. The direct reaction Hg+HCl is too slow to be of any importance here. The reaction Hg+HOCl is also slow.

The subsequent oxidation of HgCl to $HgCl_2$ can occur via any of the three following reactions, all of which are near the collisional limit:

$$HgCl + Cl_2 \rightarrow HgCl_2 + Cl \quad (5.6)$$
$$HgCl + Cl \rightarrow HgCl_2 \quad (5.7)$$
$$HgCl + HOCl \rightarrow HgCl_2 + OH \quad (5.10)$$

The principal uncertainty is in the fraction of Reaction 5.7 which branches into the products $Hg+Cl_2$.

Thus, most of the relevant reactions have rates that are near the collisional limit. The critical issue is then to include accurate chlorine chemistry.

To do this, a mechanism was assembled using the $H_2/O_2/CO/CO_2$ reaction set from Warnatz *et al.* (1996) along with the reactions involving Cl, Cl_2, HCl, ClO, HOCl, from the NIST data base NIST, 1999), as shown in Table 5.2. In addition, mercury/chlorine reactions discussed above

Table 5.2
Kinetic Data from NIST Database

							A	n	E
CL	CL	M	→	CL2		M	14.400	0.0	-1.8[1]
H	CL	M	→	HCL		M	17.000	0.0	0.0
HCL	H		→	H2	CL		13.360	0.0	3.5
H	CL2		→	HCL	CL		13.930	0.0	1.2
O	HCL		→	OH	CL		3.53	2.87	3.51
OH	HCL		→	CL	H2O		7.43	1.65	-.223
O	CL2		→	CLO	CL		12.790	0.0	3.585
O	CLO		→	CL	O2		13.2	0.0	-.193
CL	HO2		→	HCL	O2		13.030	0.0	.894
CL	HO2		→	OH	CLO		13.39	0.0	-.338
CL	H2O2		→	HCL	HO2		12.800	0.0	1.951
CLO	H2		→	HOCL	H		11.78	0.0	14.1
H	HOCL		→	HCL	OH		13.980	0.0	7.62
CL	HOCL		→	HCL	CLO		12.260	0.0	.258
CL2	OH		→	CL	HOCL		12.100	0.0	1.81
O	HOCL		→	OH	CLO		12.780	0.0	4.372
OH	HOCL		→	H2O	CLO		12.255	0.0	.994
HOCL		M	→	OH	CL	M	10.250	-3.0	56.72

cm, mole, s units. Units on E are kcal/mole
[1]subsequently adjusted as discussed in the text.

were included, excepting those involving HOCl. Also, the abstraction branch of the HgCl+Cl reaction (Reaction 5.8) was ignored. All cases used the JANAF thermochemical data (Chase *et al.,* 1985). The present experimental system is modeled as a plug-flow reactor at the measured temperature profile. The calculation is initialized at the chlorine injection point with the assumption the species arriving from the flame are equilibrated at the injection temperature. The HCl is assumed to be rapidly dispersed into the post-flame gases. Note that since the HCl enters without preheating, the calculations are started with all chlorine as HCl *(i.e.*, no initial dissociation). Due to the potential for continued reaction within the sampling system during the cooling of the gases, the probe is treated as an extension of the plug-flow reactor. The probe temperature profile is calculated from heat transfer based on a constant wall temperature equal to that of the cooling medium (see Section 3). This results in a temperature profile that varies linearly from 922 to 868°C over 1.4 s in the furnace, followed by a quench to room temperature at ~5400 K/s in the probe.

The initial calculations just focused on the furnace. The results indicated no oxidation at any condition. The chlorine atom concentrations were indicated to be near their local equilibrium values while HCl made up the balance. In spite of the fact that the reaction Hg+Cl was active in oxidizing mercury, reverse reactions converting HgCl and $HgCl_2$ to Hg were sufficiently fast that no significant oxidized mercury concentration could be sustained. Thus, the kinetics were consistent with equilibrium, but apparently inconsistent with the present data and the literature data that suggest the presence of oxidized mercury at high temperature. No reasonable adjustment of kinetic rate constants was capable of changing this conclusion. Thus, we made the decision to add the probe quench region to the calculations, as discussed above.

The first results that included the probe indicated essentially complete oxidation of the mercury. The mechanism (discussed in more detail below) indicates that Cl-atom enteres the quench region of the probe at essentially the local equilibrium concentration. As the probe gases cool, the equilibrium Cl decreases, but the kinetic rate of the $Cl+Cl+M \rightarrow Cl_2+M$ reaction is too slow to allow Cl to follow equilibrium. As the gases cool, this local superequilibrium Cl concentration results in oxidation via Hg+Cl and HgCl+Cl under temperatures where the reverse disassociation reactions are hindered. The predicted Cl concentrations are, however, unrealistically high, with significant concentrations of this radical predicted to persist right down to room temperature. Following discussions with other researchers and after reviewing the literature, we came to the conclusion that the kinetic rate of the recombination reaction is very uncertain and probably too slow at low temperatures. We adjusted this rate upward to obtain agreement with the mercury oxidation data, and used this in all subsequent calculations. The adjusted rate constant for the recombination reaction is 7.7E+16 $cm^6/mole^2$-s. The following discussion is based on this adjustment, which points out the need for independent characterization of the relevant chlorine chemistry.

The results of the calculations that include the probe are shown in Figure 5.2. These indicate reasonable agreement between the data and the chemical kinetic model. Analysis of the results indicates that the entire oxidation is due to $Hg+Cl \rightarrow HgCl$ and $HgCl+Cl \rightarrow HgCl_2$. Furthermore, the entire oxidation is taking place within the temperature quench environment provided by the sample probe. Figure 5.3 shows time resolved behavior of both mercury and Cl within the quench region. At the inlet to the quench region, mercury is in its elemental equilibrium state. The shallow temperature decline in the furnace causes a decrease in equilibrium Cl, while kinetic constraints on recombination maintain the calculated Cl somewhat above the equilibrium value at the probe inlet.

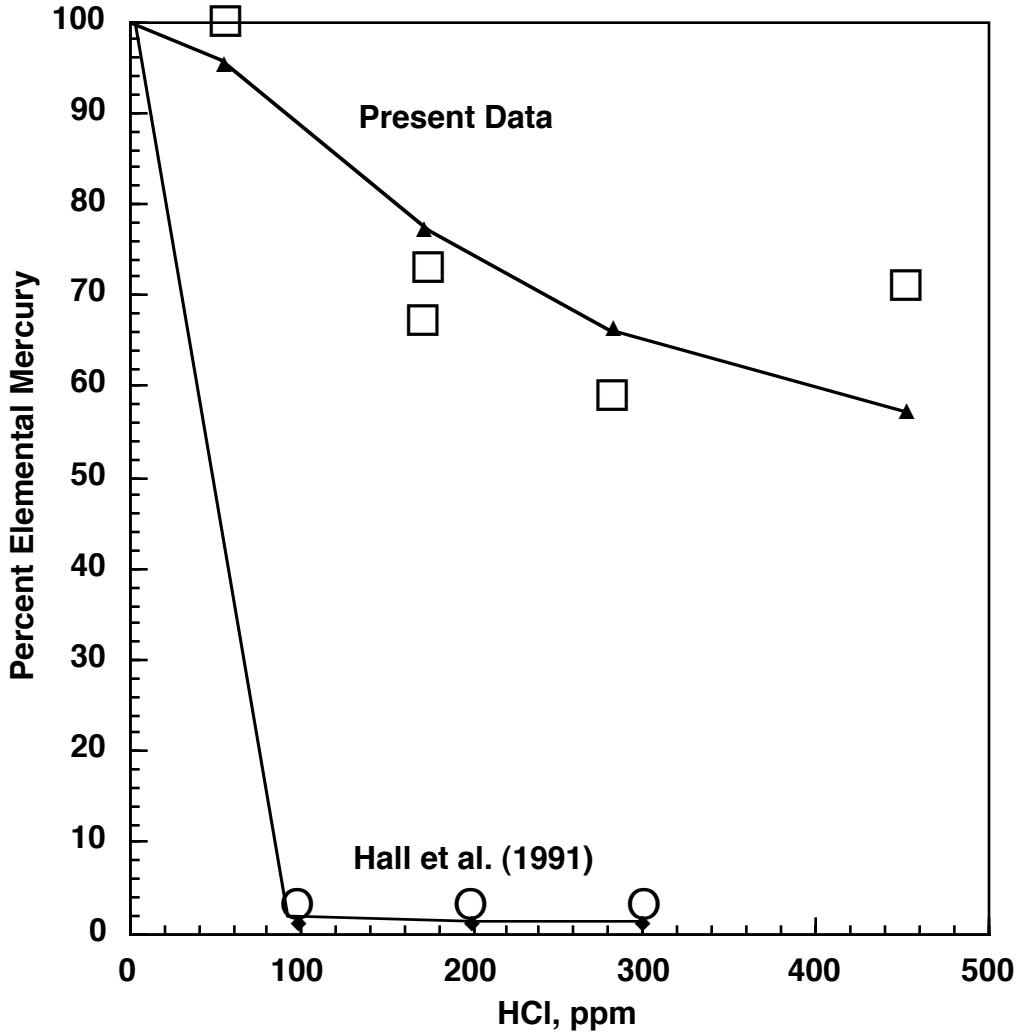

Figure 5.2. Comparison of data with predictions from the kinetic model (literature, Hall *et al.,* 1991).

The rapid quench associated with the probe, coupled with kinetic constraints on recombination cause the chlorine atom to decay at a much slower rate than the rate at which the equilibrium concentration decays. This causes the Cl-atom to be at a local superequilibirium concentration during the quench. This, coupled with the slowing of the reverse of Reactions 5.2 and 5.7, leads to oxidation. Note from the figure that the oxidation proceeds within a window associated with the overlap of (1) significant superequilibrium Cl (for T>400°C), and (2) $HgCl_2$ as a favored equilibrium product (for T<700°C).

This scenario suggests that higher temperature HCl injection may lead to more oxidation, but not because the oxidation reaction proceeds at the higher temperatures. Rather, the higher temperatures may lead to higher local Cl-atom concentrations that may not follow equilibrium well as the furnace gas temperature is quenched. This would result in higher Cl-atom concentrations being available in the quench zone, yielding more oxidation. Alternately, if the Cl-atom follow equilibrium well at higher temperatures, and its recombination becomes kinetically

constrained only at lower temperatures, then oxidized mercury yields would be independent of flame temperature or the temperature at which HCl is injected, as long as the temperature exceeds a critical value.

The influence of quench rate was investigated by repeating the calculation while adjusting the quench rate downward from the 5400 K/s that is characteristic of the probe. (Note that the lower quench rates shown on the figure encompass rates found in practical furnaces.) The results, shown in Figure 5.4, indicate that slower quench initially leads to increased oxidation, followed by reduced oxidation. Analysis of the kinetics shows that very short quench times limit the oxidation via reduced time available for reaction. Very long times allow the Cl to more closely follow equilibrium, effectively reducing the imbalance between oxidation and reduction directions of Reactions 5.2 and 5.7.

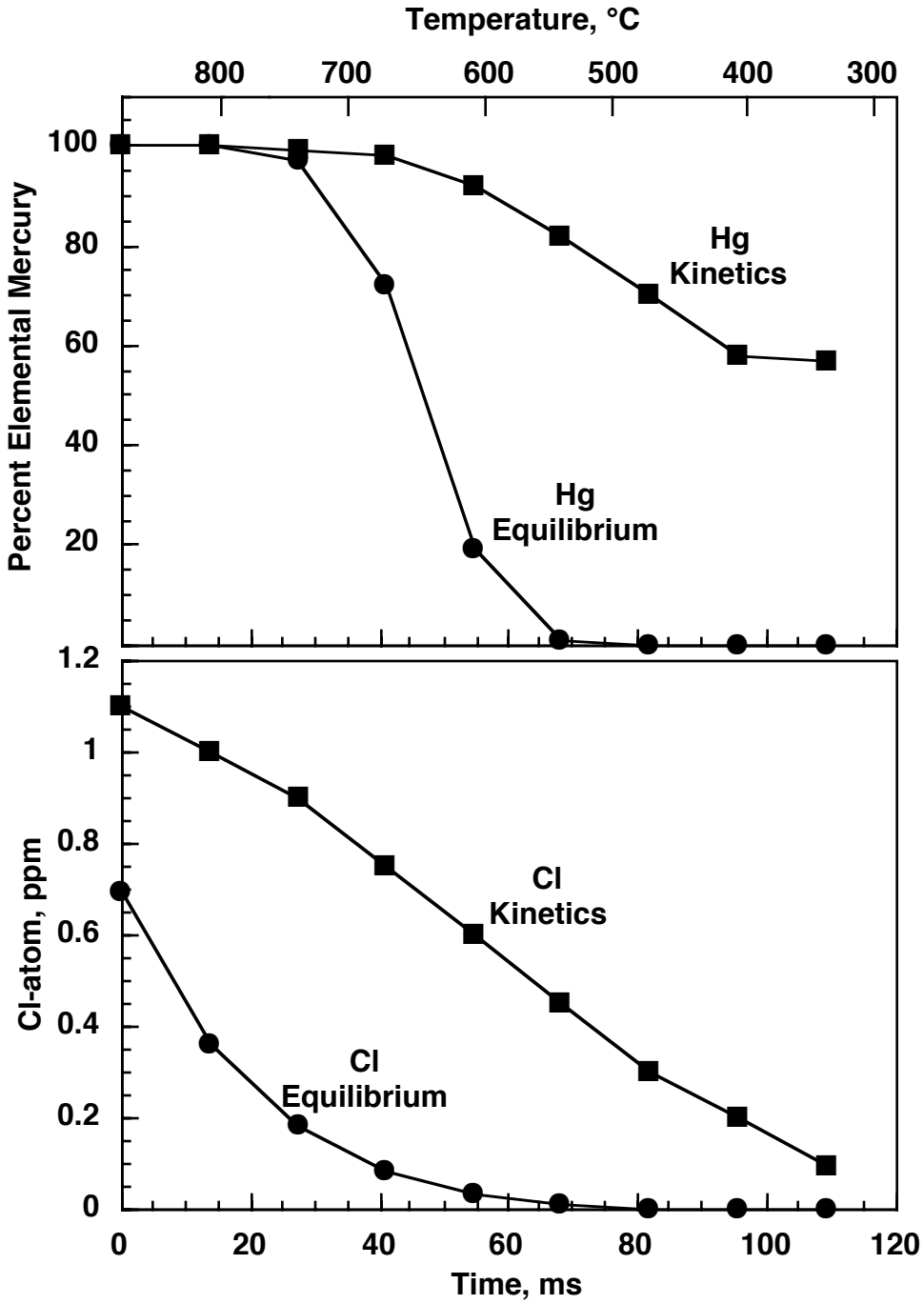

Figure 5.3. Time resolved predictions within the quench zone for the 922°C, 453 ppm initial HCl case.

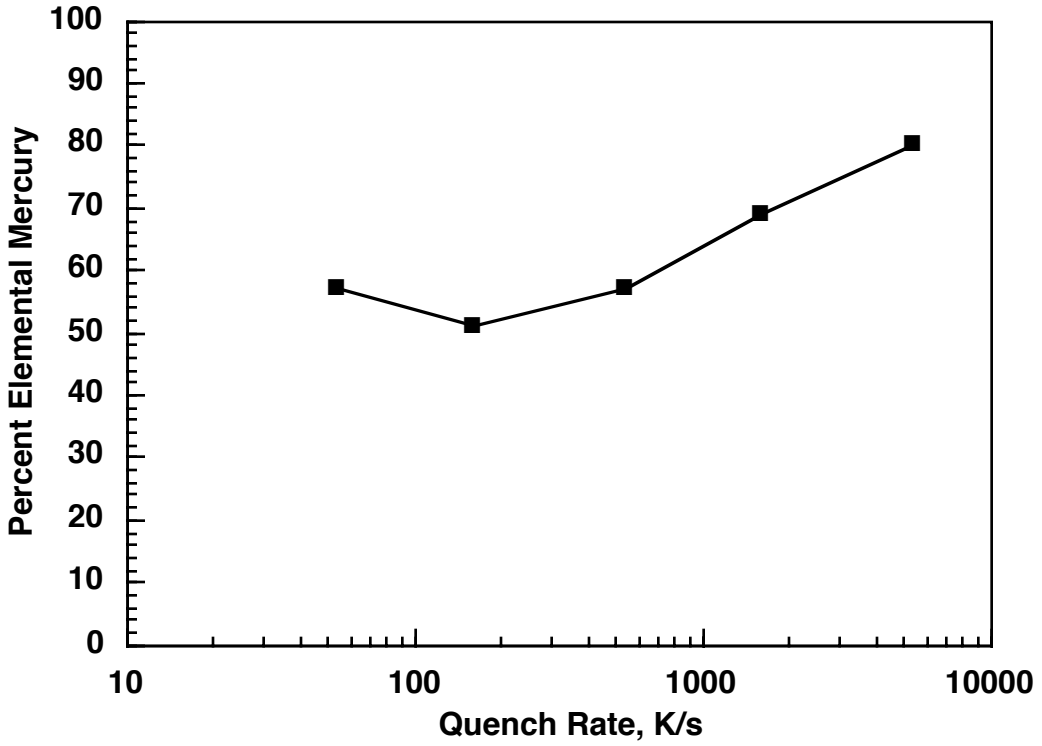

Figure 5.4. Chemical kinetic model results on the influence of quench rate on mercury oxidation.

This suggests that mercury oxidation behavior is almost exclusively dependent on the chemistry of the trace chlorine species derived from HCl. The principal reaction forming Cl-atom is:

$$OH + HCl \rightarrow Cl + H_2O \qquad (5.11)$$

This reaction is fast at the 922°C condition and almost instantaneously results in the establishment of an equilibrium concentration of Cl-atom. The amount of Cl-atom generated will depend on the maximum temperature experienced by the gas. A low temperature will reduced the rate of Reaction 5.11, as well as reducing the equilibrium Cl-atom concentration. This is consistent with the data of Hall *et al.* (1991) in which the apparent oxidation was reduced at lower reactor temperatures.

The principal reaction removing Cl is the recombination $Cl+Cl+M \rightarrow Cl_2+M$, and the results are most dependent on the rate constant of this reaction. Unfortunately, as mentioned above, this rate has not been well characterized at low temperatures, and thus this rate is thought to be the greatest source of uncertainty in the mechanism. The recombination yields Cl_2, which can react with mercury according to Reaction 5.6. There is, however, insufficient time for Reaction 5.6 to make use of this Cl_2 for oxidation under the current configuration. A long residence time at 300 K following the quench could, however, lead to more oxidation. Given the uncertainty in the rate constants, it is premature to rule out a potential mechanism in which a quench produces Cl_2 from

Cl-atom recombination, and the Cl_2 oxidized mercury near room temperature. The present rate constants, however, support the Cl-atom oxidation route.

These results then support the following hypothetical scenario:

- At high temperature (>800°C), mercury exists in the elemental form. This is due to the instability of $HgCl_2$ under these conditions. Note that this implies that at the outlet of the high-temperature portion of Hall's reactor, no oxidized mercury exists, even though the measurement suggests almost complete oxidation. This hypothesis is consistent with equilibrium.
- At the same point, Cl-atom concentrations are near their equilibrium value.
- During thermal quench, a kinetic limit on recombination leads to the actual Cl-atom concentration decaying at a much slower rate than the equilibrium concentration. This results in a local superequilibrium in Cl-atom.
- When the temperature has been reduced to the point where $HgCl_2$ is no longer unstable, mercury is oxidized via Hg+Cl and HgCl+Cl.
- The possibility remains that reactions with Cl_2 (produced by Cl-atom recombination) can also occur at low temperatures, but these are not presently indicated for our conditions.

This scenario suggests that all the oxidized mercury in the Hall experiments is generated within the cool-down region between the hot reactor exit and the inlet to the room-temperature measurement apparatus. Since all mercury analysis is presently done at room temperature, the combustion gases must pass through a quench before being characterized, and our hypothesis is that this is where mercury oxidation occurs. Figure 5.4 shows that the same behavior is obtained whether this thermal quench is at a rate characteristic of a sample probe, or similar to that occurring within a boiler.

Figure 5.2 also shows model results for the Hall *et al.* (1991) experiment. The calculations were obtained with the assumptions (1) that the product gases from the isothermal zone were cooled before the analyzer at the same rate as in the present experiment (5400 K/s), and (2) that the reacting gases were equilibrated in the high-temperature furnace. Since the reactants contain just Hg, O_2, N_2 and HCl, the only water present was the result of HCl decomposition. In this environment, the equilibrium Cl concentration is substantially higher than in the present experiment. For example, at 900°C and 300 ppm HCl, equilibrium under the present experimental composition yields 0.54 ppm Cl, while under the Hall experiment the yield is 21 ppm. This is the cause of the much higher oxidation noted in the model runs. As with the model of our experiment, all the oxidation is occurring during sample quench.

Thus, the model provides an explanation for the two principal inconsistencies noted at the start of the study. First, the observation of apparent oxidation at high temperature (contradicting equilibrium) is due to the fact that the oxidation actually occurs during the quench. Thus, the actual reaction occurs under conditions where equilibrium favors oxidation. Second, the apparent

higher reactivity of the Hall experiment is due to the use of an artificial atmosphere that lacks H_2O. This leads to significantly higher Cl-atom concentrations at the start of the quench process, which results in more oxidation.

In the experiment of Mamani-Paco and Helble (2000) the HCl was added to the mixing chamber following the flat flame. This resulted in essentially no mercury oxidation, which is inconsistent with the other experimental data reported under comparable conditions. At present, we can do no more than speculate on the possible reasons for this. It may be, however, that the mixing rate of the HCl stream into the gases was insufficient to allow the HCl to experience a high enough temperature to form sufficient Cl to drive the oxidation. Further testing is expected to resolve this issue.

6.0 Conclusions and Recommendations

The potentially high cost of custom mercury emissions control measures may be a critical problem for utility industry members should they become subject to emission regulation. A significant amount of mercury reduction has been found to occur within equipment designed to capture other pollutants, most notably FGD equipment. Oxidized mercury is water-soluble and has been shown to be much more susceptible to removal by this equipment. Thus, promoting mercury oxidation within the plant upstream of FGD equipment is one means of improving capture.

Equilibrium shows that mercury oxidation should be favored by low temperatures. Data from combustion systems and flow reactors consistently show, however, that oxidation by HCl is apparently favored by higher temperature. We have attempted to resolve this inconsistency by developing a chemical kinetic mechanism based on elementary reaction steps. These are obtained from the fundamental literature wherever possible, or from fundamental reaction rate estimates where data are not available. It was necessary to adjust the rate of the $Cl+Cl+M \rightarrow Cl_2+M$ reaction upward to match the targeted mercury oxidation data sets, but the adjustment was warranted by unrealistic Cl atom behavior at low temperatures with the literature rate constant. The mechanism supports a hypothetical scenario in which the oxidation occurs during the thermal quench of the hot gas from the reactor or furnace down to temperature where the measurement takes place (~300 K). Thus, oxidation values that are attributed to high temperatures are, in reality, indicated as having no actual oxidation at the reported temperature. This implies that the oxidation occurs within the sample system when sampling at high temperatures, and within the heat extraction region within a boiler.

The mechanism suggests that Cl-atom is at equilibrium under high temperatures. During quench, the equilibrium concentrations of Cl-atom fall quickly, but kinetic constraints on the recombination of Cl to Cl_2 keep the Cl-atom concentration high. This results in a local superequilibrium in Cl-atom as the gases cool. This drives the oxidation via Hg+Cl and HgCl+Cl. Examination of possible elementary reactions indicates that only reactions with Cl are fast enough to account for the oxidation.

Chemical kinetic modeling of the reaction environment, including the inevitable quench that must precede analysis (which occurs either in a probe or in the furnace), suggests that the oxidation occurs within a window between 700 and 400°C that is the result of the overlap of (1) a region of superequilibrium Cl concentration, and (2) a region where oxidized mercury is favored by equilibrium. The implication of these results are that homogeneous oxidation is governed primarily by (1) HCl concentration, (2) quench rate, and (3) background gas composition. The latter point is illustrated by the almost dry Hall data, where equilibrium Cl concentration are substantially elevated above those in the present experiment, resulting in much more oxidation. It also suggests that adding chlorine to improve oxidation will be most effective if the chlorine is exposed to a high-temperature environment, as observed in field data (Gleiser and Felsvang, 1994).

7.0 References

Akers, D., and Dospay, R., "Overview of the Use of Coal Cleaning to Reduce Air Toxics", *Mineral and Metallurgical Processing* **10(3),** 124-127 (1993).

Agency for Toxic Substances and Disease Registry (ATSDR), "Toxicological profile for mercury.", U.S. Department of Health and Human Services, Public Health Service. CAS # 7439-97-6, http://atsdr.cec.gov:8080/tfacts46.html (September 1995).

Becke, A.D., "Density-Functional Exchange-Energy Approximations with Correct Asymptotic Behavior", *Phys. Rev. A*. **38,** 3098-3100 (1988).

Becke, A.D., "Density-Functional Thermochemistry. III. The Role of Exact Exchange", *J. Chem. Phys*. **98,** 5648-5652 (1993).

Bergan, T., Gallardo, L., and Rodhe, N., *Atmospheric Environment* **33,** 1575-1585 (1999).

Boron, D.J., and Wan, E.I., *Coal* **96(6),** 121 (1990).

Brown, T. D., Smith, D. N., Hargis, R. A., and O'Doud, W. J., *Journal of the Air and Waste Management Association* **49,** 628-640 (1999).

Carpo. A. *Water, Air, and Soil Pollution* **98,** 241-254 (1997).

Cavallaro, J. A., Deurbrouch, A. W., Schultz, H., Gibbon, G. A., and Hattman, E. A., "A Washability and Analytical Evaluation of Potential Pollution from Trace Elements in Coal", EPA-600/7-78-038 (1978).

Chase, M.W., Jr., Davies, C.A., Downey, J.R.,Jr., Frurip, D.J., McDonald, R.A., and Syverud,A.N., "JANAF Thermochemical Tables," *J. Phys. Chem. Ref. Data* **14,** Suppl. 1 (1985).

Chow, W., and Torrens, I.M., "Managing Power Plant Trace Substances Emissions: An Overview", *Proceedings of the American Power Conference* **56(1),** 427 (1994).

Chu, P., Porcella, D.B., "Mercury Stack Emissions from U.S. Electric Utility Power Plants", *Water, Air and Soil Pollution.* **80,** 135-144 (1995).

Cole, J. D., Morgan, T. J., Nichols, R. H., and Maxwell, W. H., "Development of an Internet-Based Data Collection System for the Electric Utility Steam Generating Unit Mercury Emission Information Collection Effort", *93rd Annual Conference of the Air and Waste Management Association,* Paper No. 254, Salt Lake City, UT (June 2000).

Connors, K.A., *Chemical Kinetics*, p. 200, VCH Publishers, Inc.: New York (1990).

Devito, M., Rosendale, L., Conrad,V., and Jackson, B., "Trace Elements in Coals and their Emissions.", *Proceedings of the American Power Conference*, 56-1, 438 (1994).

Durham, M. D., Roberts, D. L., Schlager, R. J., Carter, T. G., and French, P. D., 13th *International Conference on Incineration and Thermal Treatment Technologies*, Houston, TX (May 1994).

Energy & Environmental Research Center, "Mercury Speciation Measurement Project Continuing at the EERC", *Center for Air Toxic Metals Newsletter*. **2(2),** (June 1996).

Environmental Protection Agency, "Mercury Study Report to Congress: Overview", http://www.epa.gov/oar/mercover.html (December 1997).

Environmental Protection Agency, EPA Emissions Test Method 29, "Determination of Metals Emissions from Stationary Sources", EPA-454/R-94-016 (April 1994).

Frisch, M.J., Trucks, G.W., Schlegel, H.B., Scuseria, G.E., Robb, M.A., Head-Gordon, M., Gill, P.M.W., Wong, M.W., Foresman, J.B., Johnson, B.G., Gomperts, R., Andres, J.L., Raghavachari, K., Binkley, J.S., Gonzales, C., Martin, R.L., Fox, D.J., DeFrees, D.J., Baker, J., Repologle, E.S., and Pople, J.A., *GAUSSIAN98 Rev. A.4*; Gaussian, Inc.: Pittsburgh, PA (1998).

Fthenakis, V.M., Lipfert, F. W., Moskowitz, P. D., and Saroff, L., "An Assessment of Mercury Emissions and Health Risks from a Coal-Fired Power Plant", *Journal of Hazardous Materials.* **44,** 267-283 (1995).

Galbreath, K. C., Zygarlicke, C. J., and Toman, D. L.*, 91st Annual Conference of the Air and Waste Management Association*, San Diego, CA (1998).

Ghorishi, B., and Gullet, B. K., "Sorption of Mercury Species by Activated Carbon and Calcium Based Sorbents: Effect of Temperature, Mercury Concentration and Acid Gases*", Waste Management & Research* **6,** 582-593 (1998).

Ghorishi, B. S., Lee, W. C., and Kilgroe, J. D., "Mercury Speciation in combustion Systems: Studies with Simulated Flue gases and Model Fly Ashes", *92nd Annual Conference of the Air and Waste Management Association*, St. Louis, MO (1999).

Gleiser, R., and Felsvang, K, "Mercury Emission Reduction using Activated Carbon with Spray Dryer Flue Gas Desulfurization", *Proceedings of the American Power Conference*. **56,** 452-457 (1994).

Guijarro, M. I., Mendioroz, S., and Munoz, V., "Effect of Morphology of Sulfurized Materials in the Retention of Mercury from Gas Streams", *Ind. Eng. Chem. Res.* **37,** 1088-1094 (1998).

Gullett, B.K., "Sorbent Injection for Dioxin/Furan Prevention and Mercury Control.", *Multipollutant Sorbent Reactivity Workshop*, Research Triangle Park, North Carolina (July 1994).

Gullett, B. K., Ghorishi, B., Keeney, R., and Huggins, F. E., "Mercuric Chloride Capture by Alkaline Sorbents, *93rd Annual Conference of the Air and Waste Management Association*, Paper No. 259, Salt Lake City, UT (June 2000).

Hall, B., Lindqvist, O., and Ljungström, E., "Mercury Chemistry in Simulated Flue Gases Related to Waste Incineration Conditions", *Envrion. Sci. Technol.* **24,** 108-111 (1990).

Hall, B. Schager, P., Lindqvist, O., "Chemical Reactions of Mercury in Combustion Flue Gases", *Water, Air and Soil Pollution*. **56,** 3-14 (1991).

Hassett, D. J. and Eylands, K. E., *Fuel* **78,** 243-248 (1999).

Horne, D.G., Gosavi, R., and Strausz, O.P., "Reactions of Metal Atoms. I. The Combination of Mercury and Chlorine Atoms and the Dimerization of HgCl", *The Journal of Chemical Physics*, **48,** 4758-4764 (1968).

Hranisavljevic, J., and Fontijn A., "Kinetics of Ground-State Cd Reactions with Cl_2, O_2, and HCl over Wide Temperature Ranges," *J. Phys. Chem.* **101,** 2323-2326 (1997).

Hsu, H.-C., Rostam-Abadi, M., Rood, M. J., Chen, S., and Chang, R., "Preparation of Sulfur-Impregnated Activated Carbon Fibers (ACFs) for Removal of Mercury Vapor from Simulated Coal-Combustion Flue Gases", *93rd Annual Conference of the Air and Waste Management Association*, Paper No. 435, Salt Lake City, UT (June 2000).

Jones, C., "Consensus on Air Toxics Eludes Industry to Date", *Power*: 51-59 (October 1994).

Karatza, D., Lancia, A., and Musmarra, D., "Fly Ash Capture of Mercuric Chloride Vapors from Exhaust Combustion Gas", *Environ. Sci. Technol.* **32,** 3999-4004 (1998).

Krivanek, C., "Mercury Control Technologies for MWCs: The Unanswered Questions", *Journal of Hazardous Materials*. **47,** 119-136 (1996).

Laudal, D. L., Heidt, M. K., Galbreath, K. C., Nott, B. R., and Brown, T. D., "State of the Art: Mercury Speciation Measurement in Coal Combustion Systems", *90th Annual Conference of the Air and Waste Management Association*, Toronto (June 1997).

Lee, C., Yang, W., and Parr, R.G., "Development of the Colle-Salvetti Correlation-Energy Formula into a Functional of the Electron Density," *Phys. Rev. B* **37,** 785-789 (1988).

Lee, C. W., Kilgroe, J. D., and Ghorishi, S. G., *Proceedings of the 6th Annual Waste-to-Energy Conference*, Miami Beach, FL 221-238 (1998).

Lee, C. W., Kilgroe, J. D., and Ghorishi, S. G., "Speciation of Mercury in the Presence of Coal and Waste Combustion Fly Ashes", *93rd Annual Conference of the Air and Waste Management Association*, Paper No. 584, Salt Lake City, UT (June 2000).

Lin, C. J., and Pehkonen, S. O., "The Chemistry of Atmospheric Mercury: A Review", *Atmospheric Environment* **33,** 2067-2079 (1999).

Linak, W. P., U.S. EPA Air and Energy Engineering Research Laboratory, Research Triangle Park, N.C., personal communication (June 29, 1998).

Liu, W. Radisav, D. V., and Brown, T. D., *Environmental Science and Technology* **32,** 531-538 (1998).

Mamani-Paco, R. M., and Helble, J. J., "Bench-Scale Examination of Mercury Oxidation under Non-Isothermal Conditions", *93rd Annual Conference of the Air and Waste Management Association*, Paper No. 584, Salt Lake City, UT (June 2000).

Masuda, S. In: *Managing Hazardous Air Pollutants: State of the Art*, Chow, W. and Connor, K. K. eds., EPRI TR-101890, Lewis Publishers, Boca Raton, LA (1993).

Meij, R., "The Fate of Mercury in Coal-fired Power Plants and the Influence of Wet Flue-gas Desulphurization", *Water, Air and Soil Pollution*. **56,** 21-33 (1991).

Mendioroz, S., Guijarro, M. I., Bermejo, P. J., and Munoz, V., "Mercury Retrieval from Flue Gas by Monolithic Absorbents Based on Sulfurized Sepriolite", *Environ. Sci. Technol*. **33,** 1697-1702 (1999).

Miller, S. J., Olson, E. S., Dunham, G. E., Sharma, R. K., "Preparation Methods and Test Protocol for Mercury Sorbents", *91st Annual Conference of the Air and Waste Management Association*, San Diego, CA (June 1998).

Morency, J. R., Panagiotou, T., and Senior, C. L., "Laboratory Duct Injection of a Zeolite-Based Mercury Sorbent", *93rd Annual Conference of the Air and Waste Management Association*, Paper No. 610, Salt Lake City, UT (June 2000).

NIST Chemical Kinetic Database: http://www.cstl.nist.gov/div836/ckmech.html/ (1999).

Norton, G. A., Yang, H., Brown, R. C., Laudal, D. L., Dunham, G. E., and Okoh, J. M., "Effects of Fly Ash on Mercury Oxidation in Simulated Flue Gas Environments", *93rd Annual Conference of the Air and Waste Management Association*, Paper No. 167 , Salt Lake City, UT (June 2000).

Pai, P., Niemi, D., and Powers, W., "A North American Inventory of Anthropogenic Mercury Emissions", *93rd Annual Conference of the Air and Waste Management Association*, Paper No. 450, Salt Lake City, UT (June 2000).

Richardson, C., Blythe, G., and Rhudy, R., "Enhanced Control of Mercury by Wet FGD Systems", *93rd Annual Conference of the Air and Waste Management Association*, Paper No. 43, Salt Lake City, UT (June 2000).

Rizeq, R., Hansell, D., and Seeker,W., "Predictions of metals emissions and partitioning in coal-fired combustion systems", *Fuel Processing Technology*. **39,** 219-236 (1994).

Senior, C. L., Bool, L. E., Huffman, G. P., Huggins, F. E., Shaw, N., Sarofim, A., Olmez, I, and Zeng, T., "A Fundamental Study of Mercury Partitioning in Coal Fired Power Plant Flue Gas", *Air & Waste Management Association's 90th Annual Meeting and Exhibition*, 97-WP72B.08 (June 1997).

Senior, C. L., Sarofim, A. F., Zeng, T., Helble, J. J., and Mamani-Paco, R., "Gas-Phase Transformations fo Mercury in Coal-Fired Power Plants", *Fuel Processing Technology* **63,** 197-213 (2000).

Serre, S. S., Gullett, B. K., and Ghorishi, S. B., "Elemental Mercury Capture by Activated Carbon in a Flow Reactor", *93rd Annual Conference of the Air and Waste Management Association*, Paper No. 261, Salt Lake City, UT (June 2000).

Standard Methods for Water and Wastewater Analysis, Method 303F, "Determination of Mercury by the Cold Vapor Technic", 15th Edition.

Steinfeld, J.I., Francisco, J.S., and Hase, W.L., *Chemical Kinetics and Dynamics,* Second Edition, p. 300, Prentice-Hall, New York (1999).

Wadt, W.R., and Hay, P.J., "*Ab initio* Effective Core Potentials for Molecular Calculations. Potentials for Main Group Elements Na to Bi", *J. Chem. Phys*. **82,** 284-296, (1985).

Warnatz, J., Maas, U., and Dibble, R.W., *Combustion,* Springer Publishing Company, 67-71 (1996).

Widmer, N. C., Cole, J. A., Seeker, W. R., and Gaspar, J. A., *Combust. Sci. Technol***, 134,** 315-326 (1998).

Widmer, N. C., West, J., and Cole, J. A., "Thermochemical Study of Mercury Oxidation in Utility Boiler Flue Gases", *93rd Annual Conference of the Air and Waste Management Association,* Paper No. 390, Salt Lake City, UT (June 2000).

Zhuang, Y., Biswas, P., Quintan, M. E., Lee, T. G., Arar, E., "Kinetic Study of Adsorption and Transformation of Mercury on Fly Ash Particles in an Entrained Flow Reactor", *93rd Annual Conference of the Air and Waste Management Association*, Paper No. 331, Salt Lake City, UT (June 2000).

Appendix A
Furnace Operations Checklist

Main Burner Startup

Date: Time:

Check that all valves to water lines are open.	
Isoprobe and HCl Injector coolant water rotometers > 100 mm	
Check that coolant air is running	
Exhaust fan set on "FAST"	
Turn on Main Air Supply (on wall) with regulator pressure about 50 psig	
Turn on Natural Gas Supply and Main Burner Natural Gas (on wall)	
Turn safety panel main power switch to ON. (white light)	
Check that Hg Injection Air is off.	
Press manual override button on safety panel and set natural gas to 10	
Set Main Burner Air at about 3 on rotometer.	
Remove ignition port plug and light torch	
Controller - push and hold ignition button, Lighter - move flame into burner Controller-green light, release ignition button, Lighter-flame, replace ignition port plug If flame goes out Controller presses Reset and repeat procedure.	
Adjust furnace conditions to NG = 35, Air = 22 (pressure around 44 psig)	
Adjust Hg Injection Air to 30 psig, 30 mm (lower if furnace sounds like it may go out)	
Next day: Adjust furnace conditions to NG = 62, Air = 35 (pressure around 42)	
If duct temp is getting high (> 100 F) , adjust cooling water to about 10 mm.	

Backfire Burner Startup

Upper BF Burner Date: Time:
Lower BF Burner Date: Time:

	U	L
Turn Air Valve for the appropriate BF Burner on the control panel to ON		
Check that air flow is possible in both rotometers, then turn to 0.		
Clean lenses of IR Flame Detectors and hook up.		
Remove ignition port plugs from BF burners		
Note exhaust duct temperature and increase coolant water to 20 (BF1) or 30 (BF2)		
Turn on appropriate BF unit NG feed ball valve (on wall)		
Turn All BF Burner NG valve on the control panel to ON		
Press manual override button on safety panel and set natural gas to 20		

Controller - push and hold ignition button, Lighter - move flame into burner Controller-green light, release ignition button, If flame goes out Controller presses Reset and repeat procedure.		
Turn up air to 115 on both rotometers		
Replace ignition port plugs.		
Check exhaust duct temp. Try to run less than 110 F. Furnace shuts off @130 F.		

Furnace Shutdown

Date: Time:

Turn off natural gas (NG) supply ball valve on wall.	
Turn off upper and lower backfire NG ball valves on wall.	
Turn All BF burner NG valve on the board to OFF	
Turn off backfire burner NG rotometers on board.	
Turn off main burner NG ball valve on wall.	
Turn off main burner NG rotometers on board.	
Turn all knobs on control panel to OFF.	
Allow air and water to continue running, to cool furnace and probes.	
Disconnect IR sensors from backfire burners and main burner	
Turn off the main & BF air valve on wall	
Turn off upper and lower BF valves on board	
Turn off main air, cooling air, BF and Hg injection rotometers	
Turn off water valve at wall.	
Turn off isoprobe, fuel injector and duct coolant rotometers	
Turn exhaust fan to slow	
Unplug box fan and above furnace ventilation	

Appendix B
Run and Post-Run Procedure Checklists for the Two Mercury Analytical Methods

Run Checklist (UW Med Lab)

Date:

Make KMnO4/H2SO4 solution.	
Put ice in ice bath.	
Load mercury syringe.	
Assemble Impingers 5 and 6.	
Take pre-test temperature profile.	
Hook up probe bath	
Start HCl injection _____ minutes before run	
Hook up leads to probe/impingers.	
Start Hg injection 5 minutes before run.	
Reset dry test meter.	
Make sure pre-pump valve is closed.	
Start pump and immediately open pre-pump valve.	
Adjust rotometer flow to 55.	
Run test for 4 hours, checking test conditions periodically.	
Shut pre-pump valve and immediately stop pump.	
Disassemble leads to probe/impinger.	
Remove probe and allow to cool.	
Cover ends of lead and probe with Seran Wrap.	

Post-Run Checklist (UW Med Lab)

Run Date:

Rinse probe and Teflon tube with Acetone and transfer washings to a 250 ml beaker	
Evaporate contents of beaker to dryness using fan (about 2 days).	
Rinse probe and Teflon tube with HNO3 and transfer washings to Container #3	
Filter KMnO4/H2SO4 solution using a Whatman 541 filter.	
Measure contents of each of Impingers 1 - 3 and transfer to Container #4	
Clean first three impingers and connecting glassware with 100ml 0.1 N HNO3 and add to Container #4. Record final volume of Container #4.	
Remove sample from Container #4 and label as **Analytical Fraction 2B**	
Measure contents of Impinger 4 and put in Container #5A.	

Rinse Impinger 4 with 100ml of 0.1N HNO3 and put in Container #5A.	
Remove sample from Container #5A and label as **Analytical Fraction 3A**	
Measure contents of Impingers 5 and 6 and put in Container #5B.	
Rinse both impingers and connectors with 100 ml of KMnO4. Add to Container #5B.	
Rinse both impingers and connectors with 100 ml of water. Add to Container #5B.	
Put 200ml of water in Container #5C.	
Use 25 ml of 8 N HCl to remove deposits from the impingers and connecting glassware. Put washings in Container #5C.	
Weigh the Silica Gel Impinger	
Dissolve the residue from Container #2 beaker using 10 ml of concentrated HNO3 and add to Container #3.	
Pour contents of Container #3 into original Container #2 beaker.	
Reduce contents of Containers 2/3 to about 20 ml using a hot plate.	
Put contents of Containers 2/3 into a microwave pressure relief vessel.	
Add 6 ml of concentrated HNO3 and 4ml of concentrated HF	
Microwave the sample, following the Method 29 instructions.	
Filter contents of Containers 2/3 using Whatman 541 filter paper.	
Dilute contents of Containers 2/3 to 100ml	
Remove sample from Containers 2/3 and label as **Analytical Fraction 1B**	
On the day the UW Medical Lab is ready:	
Filter contents of Container #5B through Whatman 40 filter paper into a 500ml volumetric flask and dilute to volume with water.	
Remove sample from Container #5B volumeteric flask and label as **Fraction 3B**. **Note: Analytical Fraction 3B must be analyzed within 48 hours at the lab.**	
Put filter paper in a vented container	
Using a hood, add 25 ml of 8 N HCl to filter and allow to digest for a min of 24 hours	
Take **Analytical Fractions 1B, 2B, 3A and 3B** to the UW Medical Lab	
Filter contents of Container #5C through Whatman 40 filter into a 500 ml flask.	
Filter the results Container #5B filter digestion through the same filter into the flask.	
Dilute of volume and mix.	
Remove sample from flask and label as **Analytical Fraction 3C**	
Take **Analytical Fraction 3C** to lab with set of samples.	

Run Checklist (AmTest)

Date:

Make $KMnO_4/H_2SO_4$ solution.	
Put ice in ice bath.	
Load mercury syringe and note pre-test syringe level.	
Assemble Impingers 5 and 6.	
Write down furnace conditions and take pre-test temperature profile.	
Hook up probe bath	
Start HCl injection _____ minutes before run	
Hook up leads to probe/impingers.	
Start Hg injection 5 minutes before run.	
Reset dry test meter.	
Make sure pre-pump valve is closed.	
Start pump and immediately open pre-pump valve.	
Adjust rotometer flow to 55.	
Run test for 4 hours, checking test conditions periodically.	
Remove impingers for next run from HNO_3 bath and rinse.	
Shut pre-pump valve and immediately stop pump.	
Shut off Hg injection and note post-test syringe level.	
Shut off HCl at bottle and start air purge.	
Disassemble leads to probe/impinger.	
Remove probe and allow to cool.	
Note total test time and dry test meter reading.	
Cover ends of lead and probe with Seran Wrap.	

Post-Run Checklist (AmTest)

Date:
Run Date:

Rinse probe and Teflon tube with 100 ml Acetone.	
Transfer acetone wash to **Container #2**, mark fluid level and label.	
Rinse probe and Teflon tube with 100 ml 0.1 N HNO_3 .	
Transfer HNO_3 wash to **Container #3**, mark fluid level and label.	
Refilter $KMnO_4/H_2SO_4$ solution using Whatman 541 filter.	
Measure contents of each of Impingers 1 - 3 and transfer to **Container #4.**	
Clean first three impingers and connecting glassware with 100ml 0.1 N HNO_3.	

Add HNO_3 wash to **Container #4**, record final volume, mark fluid level and label.	
Measure contents of Impinger 4 and put in **Container #5A**.	
Rinse Impinger 4 with 100ml of 0.1N HNO_3.	
Add HNO_3 wash to **Container #5A** and label.	
Measure contents of Impingers 5 and 6 and put in **Container #5B**.	
Rinse both impingers and connectors with a total of 100 ml of $KMnO_4/H_2SO_4$.	
Add $KMnO_4/H_2SO_4$ rinse to **Container #5B**.	
Rinse both impingers and connectors with a total of 100 ml of water.	
Add the water rinse to **Container #5B** and label.	
Put 200ml of water in **Container #5C**.	
Rinse both impingers and connectors with a total of 25 ml of 8 N HCl.	
Add the HCl rinse to **Container #5C** and label.	
Weigh the Silica Gel Impinger.	
Bake Silica Gel.	
Put impingers 1-6 and connecting glassware in HNO_3 bath.	
Set up impingers 1-4 for the next run.	
Weigh the Silica Gel Impinger for the next run.	

Buck Checklist

Date:

Make $KMnO_4/H_2SO_4$ solution.	
Put ice in ice bath, refill ice trays.	
Fill mercury syringe	
Hook up syringe with vent line open to prevent pressure from adding air to syringe	
Assemble sampling train according to notebook picture.	
Write down furnace conditions and take pre-test bare TC temperature profile.	
Hook up probe bath	
Hook up leads to probe/impingers and to outside venting.	
Turn on Buck analyzer pump/power switches and allow to warm up 15 minutes.	
Calibrate Buck analyzer: Memory Off - meter %T - close shutter - adjust to 0%T - open shutter - adjust to 100%T - close shutter - adjust to 0%T - open shutter- meter x5 - adjust to 100%T	
Reset dry test meter.	
Testing:	
Make sure pre-pump valve is closed.	
Start pump and immediately open pre-pump valve.	
Adjust rotometer flow to 55 old setting (or full open about 40).	
Close Hg injection vent line. Start Hg injection water and syringe drive. Note: Shut off Hg throughout testing to	

conserve Hg solution. (i.e. when waiting for HCl injection)	
Take timed flow reading with dry test meter	
For HCl Injection:	
Ensure that nitogen purge valve is closed.	
Open HCl valve and adjust rate using valve after rotometer. Rotometer may stick.	
Allow time for the HCl to reach the furnace (20 min?)	
After testing:	
Shut off Hg injection, but leave injection water running.	
Shut off HCl at bottle. Open regulator. Open post-rotometer valve to let line clear. Close teflon HCl valve.	
Turn on nitrogen at bottle. Open teflon and stainless nitrogen valves. (press <35 psig)	
Watch Hg levels drop to 0 for Buck purge.	
Shut pre-pump valve and immediately stop pump.	
Turn off Buck analyzer pump and power.	
Disassemble leads to probe/impingers and between carts.	
Shut off water to probe bath. Remove probe and allow to cool.	
Place end of Hg vent line in an Hg waste container. Shut off injection water and open vent valve, allowing water in line to drain into container.	
Take down syringe. Dispose of excess Hg solution. Rinse syringe	
Turn off nitrogen at bottle, close teflon and stainless nitrogen valves and watch rotometer drop. Close post-rotometer valve.	

Appendix C
Statistical Analysis of Mercury Concentration Data

Test	X1 HCl (ppm)	X2 Hg (μg/m^3)	X3 % Ele	(X1)^2	(X2)^2	(X3)^2	X1*X2	X2*X3	X1*X3
1	56	53	100	3136	2809	10000	2968	5300	5600
2	172	53	67	29584	2809	4489	9116	3551	11524
3	175	53	73	30625	2809	5329	9275	3869	12775
4	282	53	59	79524	2809	3481	14946	3127	16638
5	453	53	71	205209	2809	5041	24009	3763	32163
6	0	590	100	0	348100	10000	0	59000	0
7	53	590	92.663	2809	348100	8586	31270	54671.22	4911.144
8	163	590	82.655	26569	348100	6832	96170	48766.2	13472.7
9	276	590	73.727	76176	348100	5436	162840	43498.98	20348.67
10	450	590	52.325	202500	348100	2738	265500	30871.62	23546.15
11	550	590	48.486	302500	348100	2351	324500	28606.6	26667.17
12	0	590	100	0	348100	10000	0	59000	0
13	53	590	92.663	2809	348100	8586	31270	54671.22	4911.144
14	163	590	70.971	26569	348100	5037	96170	41872.84	11568.26
15	276	590	54.357	76176	348100	2955	162840	32070.53	15002.48
16	450	590	41.632	202500	348100	1733	265500	24562.91	18734.42
17	550	590	24.422	302500	348100	596.4	324500	14408.78	13431.91
18	0	826	100	0	682276	10000	0	82600	0
19	55	826	82.655	3025	682276	6832	45430	68272.68	4546.002
20	169	826	56.468	28561	682276	3189	139594	46642.39	9543.055
21	279	826	48.486	77841	682276	2351	230454	40049.24	13527.53
22	444	826	37.135	197136	682276	1379	366744	30673.82	16488.11
23	536	826	34.411	287296	682276	1184	442736	28423.31	18444.18
24	0	826	100	0	682276	10000	0	82600	0
25	55.7	826	85.864	3102.5	682276	7373	46008.2	70924.06	4782.651
26	167	826	54.357	27889	682276	2955	137942	44898.74	9077.59
27	281	826	44.928	78961	682276	2019	232106	37110.86	12624.88
28	447	826	35.747	199809	682276	1278	369222	29527.14	15978.97
29	543	826	33.124	294849	682276	1097	448518	27360.75	17986.55
30	0	540	100	0	291600	10000	0	54000	0
31	55.7	540	76.59	3102.5	291600	5866	30078	41358.75	4266.079
32	167	540	63.305	27889	291600	4008	90180	34184.9	10572
33	281	540	50.369	78961	291600	2537	151740	27199.1	14153.61
34	447	540	44.928	199809	291600	2019	241380	24261.34	20083
35	543	540	40.076	294849	291600	1606	293220	21640.88	21761.11
36	0	590	100	0	348100	10000	0	59000	0
37	55.7	590	69.632	3102.5	348100	4849	32863	41082.71	3878.487
38	170	590	63.305	28900	348100	4008	100300	37350.17	10761.91
39	281	590	52.325	78961	348100	2738	165790	30871.62	14703.26
40	447	590	46.673	199809	348100	2178	263730	27537.19	20862.92
41	543	590	41.632	294849	348100	1733	320370	24562.91	22606.2
42	0	1390	100	0	1932100	10000	0	139000	0
43	55.7	1390	58.661	3102.5	1932100	3441	77423	81538.39	3267.402

44	170	1390	52.325	28900	1932100	2738	236300	72731.45	8895.214
45	281	1390	40.076	78961	1932100	1606	390590	55705.22	11261.27
46	447	1390	30.694	199809	1932100	942.1	621330	42664.79	13720.26
47	543	1390	26.355	294849	1932100	694.6	754770	36633.9	14310.94

∑X	11585.8	32377	2974				8049692	1952017	549397.2
avg X	246.5064	688.8723	63.277						
∑X^2	4583509	27809357	213808						

∑(x1)^2	1727535	r(1-3)=[∑(x1*x3)]/[∑x1*∑x3]^.5	=	-0.87325
∑(x1*x2)	68555.04	r(2-3)=[∑(x2*x3)]/[∑x2*∑x3]^.5	=	-0.25748
∑ (x2)^2	5505737			
∑(x1*x3)	-183718			
∑(x2*x3)	-96704			
∑ (x3)^2	25621.05			

Here:

$\sum(x1*x2) = \sum(X1*X2) - [(\sum X1)*(\sum X2)]/N$, etc.